Universidade Estadual Paulista
"Júlio de Mesquita Filho"

Faculdade de Ciências Farmacêuticas

Qualidade de água de coco embalada em filmes de polietileno de baixa densidade linear incorporadas com nanopartículas de prata

Sabrina da Costa Brito

Tese apresentada ao Programa de Pós-graduação em Alimentos e Nutrição para obtenção do título de Doutora em Alimentos e Nutrição.

Área de concentração: Ciências dos Alimentos

Orientador: Prof. Dr. Marcos David Ferreira.

Araraquara

2023

Qualidade de água de coco embalada em filmes de polietileno de baixa densidade linear incorporadas com nanopartículas de prata

Sabrina da Costa Brito

Tese apresentada ao Programa de Pós-graduação em Alimentos e Nutrição para obtenção do título de Doutora em Alimentos e Nutrição.

Área de concentração: Ciências dos Alimentos

Orientador: Prof. Dr. Marcos David Ferreira.

Araraquara

2023

Brito, Sabrina da Costa.
B862q Qualidade de água de coco embalada em filmes de polietileno de baixa densidade linear incorporadas com nanopartículas de prata / Sabrina da Costa Brito. – Araraquara: [S.n.], 2023.
109 f. : il.

Tese (Doutorado) – Universidade Estadual Paulista. "Júlio de Mesquita Filho". Faculdade de Ciências Farmacêuticas. Programa de Pós Graduação em Alimentos, Nutrição e Engenharia de Alimentos. Área de Concentração em Ciência dos Alimentos.

Orientador: Marcos David Ferreira.

1. Nanotecnologia. 2. Nanopartículas de prata. 3. Antimicrobianas. 4. Embalagens ativas. I. Ferreira, Marcos David, orient. II. Título.

Diretoria do Serviço Técnico de Biblioteca e Documentação - Faculdade de Ciências Farmacêuticas
UNESP - Campus de Araraquara

CAPES: 33004030055P6
Esta ficha não pode ser modificada

UNIVERSIDADE ESTADUAL PAULISTA
"JÚLIO DE MESQUITA FILHO"
Câmpus de Araraquara

Araraquara, 23 de junho de 2023.

Certificamos que a *Diretoria Técnica de Biblioteca e Documentação* da Faculdade de Ciências Farmacêuticas, da Universidade Estadual Paulista "Júlio de Mesquita Filho" Revisou as citações no texto e referências bibliográficas, segundo a Norma **Estilo Vancouver** da tese de doutorado de "**Sabrina Costa Brito**" do Programa de Pós-graduação em Alimentos, Nutrição e Engenharia de Alimentos, área de Concentração: Ciência de Alimentos.

Atenciosamente,

Maria Irani Coito
Diretor Técnico de Serviço
Diretoria Técnica de Biblioteca e Documentação
CRB-8/4.440

Agradecimentos

Á Fundação de Amparo à Pesquisa do Estado de São Paulo (FAPESP).

Ao Conselho Nacional de Desenvolvimento Científico e Tecnológico/MCTI-SisNano (CNPq/442575/2019-0) e ao Research Fellowship (CNPq/310728/2019-3).

À Coordenação de Aperfeiçoamento de Pessoal de Nível Superior – Brasil- CAPES (Finance Code 001).

À Empresa Brasileira de Pesquisa Agropecuária (EMBRAPA, Project 13.16.04.041.00.00) e pela Rede Agronano-EMBRAPA.

Agradeço ao professor Dr. Marcos David Ferreira pela orientação ao longo de todo o doutorado.

Também agradeço a Embrapa pecuária, a Universidade de São Carlos e a Universidade de Ribeirão Preto pela colaboração nas análises realizadas neste trabalho. E meus agradecimentos também são direcionados a empresa Green Coco Ltda, sob o nome do Mr. Gamaliel Pires de Moura por fornecer as amostras de água de coco e a empresa Nanox por fornecer os pellets de AgNPs + SiO2.

E agradeço à Faculdade de Ciências Farmacêuticas – UNESP e Embrapa Instrumentação por todo suporte e infraestrutura.

Resumo

Objetivo: Este estudo visou verificar a eficácia antimicrobiana e extensão da vida de prateleira em água de coco condicionada em filmes de polietileno de baixa densidade linear (PEBDL) aditivados com nanopartículas de prata (AgNPs) dispersas no carregador de sílica (SiO_2) e hidroxiapatita (HAP), em diferentes concentrações em porcentagem (%) por filme polimérico **Metodologia:** Na pesquisa foram estudadas três concentrações diferentes de AgNPs (%) (0,2; 0,4 e 0,6) para ambos carregadores em filmes PEBDL, além do filme controle (sem nanopartículas). Tanto os aditivos AgNPs + SiO_2 e AgNPs + HAP quanto os filmes caracterizados por: difração de raio X (DRX), espectroscopia no infravermelho com transformada de Fourier (FTIR), microscopia eletrônica de varredura (FEG-SEM), espalhamento dinâmico de luz (DLS), potencial zeta, termogravimetria (TGA) e calorimetria diferencial de varredura (DSC). A ação antimicrobiana foi pesquisada contra os seguintes microrganismos, Gram Positivo: *Staphylococcus aureus,* Gram Negativo: *Escherichia coli* e os fungos *Penicillium expansum* e *Fusarium solani*; por meio das metodologias de atividade antimicrobiana por contato e imagens bacterianas por microscopia eletrônica de varredura (MEV). Na análise de vida de prateleira de água de coco foram realizados procedimentos físico-química de pH, acidez titulável, sólidos solúveis, cor, turbidez, compostos fenólicos, açucares redutores e não redutores e minerais, e análises microbiológicas em psicrotróficos, bolores e leveduras enterobactérias e *Salmonella* spp. **Resultados:** A adição de AgNPs na matriz do PEBDL não interferiu nas propriedades químicas e térmicas dos filmes e não houve migração significante de prata para o meio externo. Em relação a atividade antimicrobiana, foi observado que a maioria das concentrações realizaram uma inibição maior de 90% em todos os microrganismos estudados, independente do carregador, entretanto uma maior ação antimicrobiana foi para bactéria Gram positiva do para que a Gram negativa e entre os carregadores, a HAP a foi mais efetiva. Com relação ao envase da água de coco em embalagens com nanotecnologia, verificou-se que, independentemente do carregador houve maior manutenção das características físico-química ao longo do período de armazenamento, correlacionando o resultado a redução da carga microbiana do produto em embalagem com AgNPs. **Conclusão:** Os resultados desta pesquisa demostraram que as embalagens com nanopartículas de prata, independente do carregador, e, mesmo em baixas concentrações são efetivas na manutenção e otimização da qualidade físico-química e microbiológicas da água de coco armazenada sob refrigeração acima de 5°C e em um período superior a 30 dias.

Palavras-Chave: nanotecnologia; nanopartículas de prata; antimicrobianas; embalagens ativas.

Abstract

Objective: This study aimed to verify the antimicrobial efficacy and extension of shelf life in coconut water conditioned in linear low density polyethylene (LLDPE) films added with silver nanoparticles (AgNPs) dispersed in the silica carrier (SiO2) and hydroxyapatite (HAP), at different concentrations in percentage (%) per polymeric film **Methodology:** In the research, three different concentrations of AgNPs (%) (0.2; 0.4 and 0.6) were studied for both carriers in LLDPE films, in addition to the control film (without nanoparticles) . Both the AgNPs + SiO2 and AgNPs + HAP additives and the films characterized by: X-ray diffraction (XRD), Fourier transform infrared spectroscopy (FTIR), scanning electron microscopy (FEG-SEM), dynamic light scattering (DLS), zeta potential, thermogravimetry (TGA) and differential scanning calorimetry (DSC). The antimicrobial action was investigated against the following microorganisms, Gram Positive: *Staphylococcus aureus*, Gram Negative: *Escherichia coli* and the fungi *Penicillium expansum* and *Fusarium solani*; through the methodologies of antimicrobial activity by contact and bacterial images by scanning electron microscopy (SEM). In the analysis of the shelf life of coconut water, physical-chemical procedures of pH, titratable acidity, soluble solids, color, turbidity, phenolic compounds, reducing and non-reducing sugars and minerals, and microbiological analyzes on psychrotrophs, molds and enterobacterial yeasts were carried out and *Salmonella* spp. **Results:** The addition of AgNPs to the LLDPE matrix did not interfere with the chemical and thermal properties of the films and there was no significant silver migration to the external environment. Regarding antimicrobial activity, it was observed that most concentrations performed a greater than 90% inhibition in all microorganisms studied, regardless of the carrier, however a greater antimicrobial action was on Gram positive bacteria than Gram negative and between carriers, PAH was more effective. Regarding the bottling of coconut water in nanotechnology packages, it was verified that, regardless of the carrier, there was a greater maintenance of the physicochemical characteristics of this product throughout the storage period, correlating this result with the reduction of the microbial load of coconut water in packaging with AgNPs. **Conclusion:** The results of this research showed that packages with silver nanoparticles, regardless of the carrier and in low concentrations, are effective in maintaining and optimizing the physical-chemical and microbiological quality of water stored under refrigeration above 5°C and in a period longer than 30 days.

Keywords: nanotechnology; silver nanoparticles; antimicrobial; active packs.

Lista de Tabelas

Lista de Figuras

Capitulo 1 **Página**

Sumário

Introdução

A comercialização da água de coco no Brasil no ano de 2020 foi de 21,9 toneladas, sendo esta bebida avaliada no mercado global em 2021 em 5 bilhões de dólares e podendo valer 11,72 bilhões de dólares em 2027, está valorização no mercado é reflexo de uma maior demanda de consumidores cientes dos benefícios do seu consumo (1,2), entretanto a água de coco é um produto que se deteriora facilmente quando exposta ao ar, sendo esta podendo ser ocasionada por atividades de microrganismos, contaminantes físicos e condições de armazenamento deficientes, além das atividades enzimáticas que é maior durante o manuseio deste produto (3–7), portanto torna atraente a incorporação de agentes antimicrobianos em garrafas plásticas de água de coco pronto para beber, assim reduzindo a sua deterioração e otimizando sua qualidade físico-química e microbiológica (8–12).

Água de Coco

O coqueiro (*Coco nucifera* L.), pertencente à família Arecaceae, é uma palmeira nativa das regiões tropicais, e amplamente cultivado na Ásia, América e África. Trazida para o Brasil na segunda metade do século XVI, tornou-se uma das mais importantes palmeiras cultivadas no país, sendo encontrado em quase todo o território brasileiro (5,13–15). O coco, cientificamente conhecido como *cocos nucifera*, é um fruto classificado como drupa fibrosa, que apresenta forma ovoide com vários tamanhos e cores (6). Em geral, um coco leva cerca de 12 meses para ficar maduro e pesa até 2 kg. Este fruto apresenta internamente duas partes comestíveis,

o núcleo branco (polpa) e o líquido claro (água de coco), e ambas podem ser processadas, fornecendo mais de 100 produtos e subprodutos (13,16).

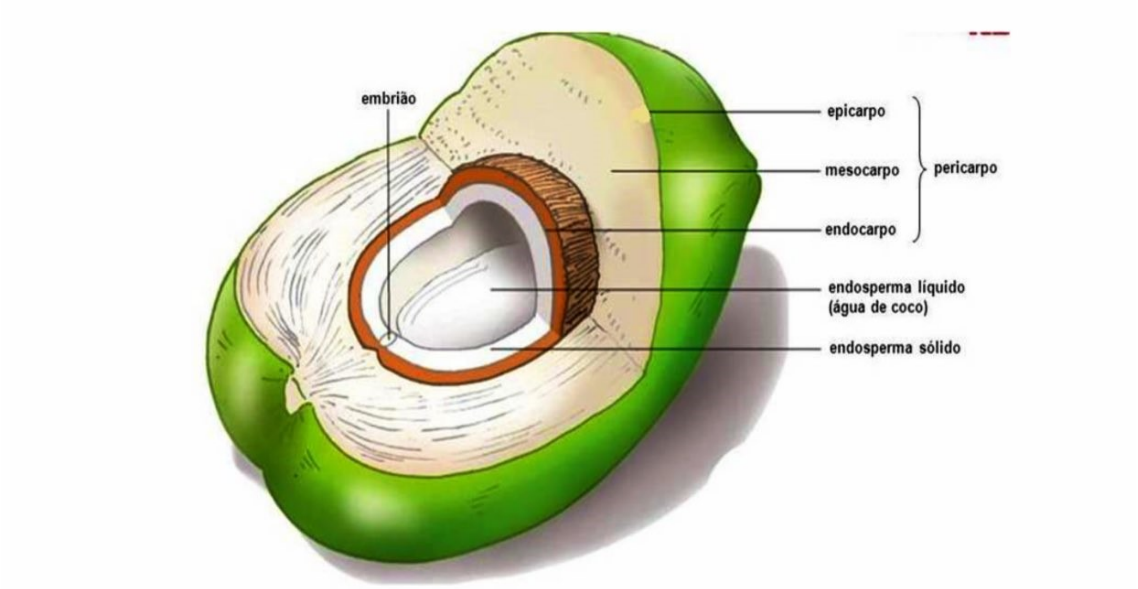

Fig. 1. Ilustração da morfologia do fruto *Coco nucifera* L. **Fonte:** Uzunian; Birner (2009)

A água de coco é um endosperma líquido que corresponde por aproximadamente 25% do peso do fruto, é uma bebida com sabor levemente adocicado e ácido, com coloração incolor (6,17,18). No terceiro mês de desenvolvimento do coco é encontrado em pequenas quantidades, mas com sete a oito meses ela atinge o máximo do seu volume (300-500 mL), e também é quando o sabor da água de coco está mais doce, este volume se mantém constante durante um ou dois meses, reduzindo até o final do madurecimento (100-150 mL) (6,14,15).

A água de coco é composta por sais minerais, proteínas e açúcares (glicose, sacarose e frutose), vitaminas e fitohormonios, sendo considerada uma bebida auxiliadora na saúde do consumidor, já que apresenta ações antioxidantes, cardioprotetor, anticancerígeno e hipoglicemiantes (17,19,20), além disso pode inibir e aliviar vários

problemas e distúrbios associados à saúde, como: diarreia, desidratação, problemas relacionados aos rins, infecção do trato urinário e entre outros (5,6,21).

Apesar de todas as suas características benéficas aos consumidores, a água de coco se deteriora facilmente quando exposta ao ar. A sua deterioração pode ser ocasionada por atividades de microrganismos, contaminantes físicos e condições de armazenamento deficientes, além das atividades enzimáticas que é maior durante o manuseio deste produto (3–7).

Em relação a sua atividade enzimática, vale ressaltar que duas enzimas se destacam, a peroxidase (POD) e a polifenol oxidase (PPO), ambas contribuem para o aparecimento de coloração rosa ou marrom na água de coco, já que são capazes de oxidar compostos fenólicos com o auxílio de oxigênio molecular, sendo está síntese relacionada como um mecanismo de defesa do fruto. O resultado final das reações catalisadas é o escurecimento enzimático, que é indesejável, já que altera o sabor, odor e valor nutricional (14,22). Portanto aspectos físico-química como acidez, turbidez, compostos fenólicos e teor de minerais, devem ser analisados com frequência, já que estão relacionados com as reações enzimáticas indesejáveis (22).

Todas estas variáveis podem causar uma diminuição da qualidade da água de coco, refletindo em uma menor vida de prateleira e perda de suas qualidades sensoriais (sabor rançoso, turbidez e pigmentos marrom) e nutricionais, além disso, pode apresentar um risco para saúde do consumidor pelo consumo de micotoxinas de fungos ou até mesmo

infecções bacterianas (6,7,23).

A preservação e o processamento da água de coco sem alterar a sua composição química e sua natureza sensorial, é o maior desafio da indústria de processamento deste produto (6,7).

Atualmente o processo para o aumento de vida de prateleira da água de coco é realizada por meio do tratamentos térmicos, como a esterilização e a pasteurização, onde a primeira elimina todos os microrganismos e seus esporos originando produtos tipo tetra pak, que não precisa ser refrigerado e tem uma vida de prateleira maior que dez meses, e a pasteurização que destrói formas vegetativas dos microrganismos a qual possibilita um tempo de prateleira de 30 dias sob refrigeração, e ambos os tratamentos inativam as enzimas peroxidase e a polifenol oxidase (ambas contribuem para o aparecimento de coloração rosa ou marrom no produto (7,24–26).

O processamento de pasteurização da água de coco resfriada, começa com a seleção e sanitização dos frutos, para posteriormente ocorrer a sua extração, geralmente está ação ocorre com o auxílio de um equipamento tipo furador de aço inox, este processo pode ser realizado por uma extratora manual ou automatizada. Nesta etapa é recomendado introduzir o equipamento na parte superior dos frutos, no pedicelo, parte que sustenta o fruto no cacho e também onde o este é gerado (15).

Com a abertura, a água é vertida em um coletor de malha ou peneira, ambas de inox, que retém as partículas ou resíduos provenientes da etapa de extração, em seguida a água é conduzida a um pasteurizador de placas, com secções de aquecimento e resfriamento, onde é submetida a

temperaturas na faixa de 90-95 °C/60 segundos e resfriada até 35 °C, por fim a água de coco é envasada, esta pode ocorrer por meio de dosadoras manuais ou semiautomáticas. O armazenamento da água de coco, deve ser em temperatura máxima de 5 °C. Com este o binômio tempo *versus* temperatura da pasteurização, a água de coco em geral não irá sofrer mudanças significativas nas suas características sensoriais durante o armazenamento em refrigeração (15,27,28).

De acordo com (28) (2017) e (29) (2004), o tratamento térmico via pasteurização, proporciona uma vida de prateleira de 30 dias em temperatura de refrigeração controlada, entretanto observou-se que nas gôndolas e estoques de supermercados esta temperatura geralmente não é seguida, podendo encontrar refrigeradores com temperaturas de 7 a 10 °C (30,31).

Com as inadequações de refrigeração, mesmo com a pasteurização a água de coco apresenta uma vida de prateleira menor que 30 dias. Salienta-se que o tratamento térmico realiza uma redução parcial da carga microbiana em uma ordem de seis ciclos decimais, sendo que pela legislação brasileira, os padrões microbiológicos aceitáveis para comercialização de sucos e outras bebidas submetidas a processos tecnológicos para redução microbiana, que necessitam de refrigeração é: *Salmonella*, ausente, Enterobacteriaceae, 10^2 e bolores e leveduras de 10^2 (28,32).

Portanto, torna-se interessante uma tecnologia aplicada a embalagem da água de coco, com a incorporação de nanopartículas metálicas em polímeros, a qual contém em sua estrutura agentes antimicrobianos que

agem na redução microrganismos no produto alimentício; adicionalmente a pasteurização a água de coco terá mais um meio de segurança para manutenção da qualidade com ação antimicrobiana, principalmente durante distribuição, onde as condições de controle de temperatura são deficientes e um possível aumento da carga microbiana é presumível (9,28).

Embalagens

A embalagem é um meio eficaz de proteção de produtos alimentícios de contaminantes externos e outras influencias (odores, choques, poeira, temperatura, danos físicos, luz, microrganismos e umidade), garantindo a prevenção de alterações químicas, físicas e biológicas (deterioração) dos alimentos, portanto é fundamental na qualidade e segurança dos alimentos, além de aumentar a vida de prateleira e minimizar o desperdício (8,10,11).

Os atributos que as embalagens devem apresentar são a compatibilidade com o produto alimentício, ser atóxico; oferecer proteção sanitária; proteger contra a passagem de umidade, gases, luz, gorduras e aromas, ser resistente a impactos físicos, ter boa aparência, ser de fácil eliminação e ter viabilidade econômica (33–36).

Dentre os materiais utilizados para embalagens, os polímeros são comumente usados para embalar alimentos, em particular os polietilenos e suas misturas, isso é devido a sua não toxicidade, alta durabilidade e facilidade de moldagem (12,37). Os exemplos de embalagens de polietileno incluem, garrafas, bandejas, tigela *bowl*, sacos, potes, filmes, *pouch*, e outros (37). Os matérias poliméricos utilizados nas embalagens

consistem, por exemplo, polietileno tereftalato (PET), polipropileno (PP), poliestireno (OS), cloreto de polivinil (PVC), polietileno de alta densidade (PEAD), polietileno de baixa densidade (PEBD) e o polietileno de baixa densidade linear (PEBDL) (37).

PEBDL, é copolímero de etileno com α-olefina (1-buteno, 1-hexeno e 1-octeno), onde uma pequena fração de α-olefina, introduz ramificações de cadeia curta, que pode proporcionar o melhoramento das propriedades mecânicas e ópticas do PEBDL, sendo que as características mecânicas deste é melhor que dos filmes feitos de PEBD e PEAD (38,39). Devido suas atraentes características, como boa flexibilidade, resistência elétrica, estabilidade térmica, alta barreira de vapor de água e excelente resistência a substancias, o PEBDL acaba sendo utilizado em muitas aplicações para embalagens de alimentos (40–42).

Bactérias e fungos, vêm ao longo dos anos sendo os responsáveis por várias doenças de origem alimentar, tornando-se uma das preocupações mais importantes na área de segurança alimentar no mundo (8). De acordo com a Organização Mundial da Saúde (OMS), em 2015, cerca de 600 milhões de pessoas foram afetadas por doenças transmitidas por alimentos e 420 mil casos de mortes pelo mesmo motivo, foram registrados no mundo todo a cada ano (8,43).

A contaminação de alimentos pode ocorrer durante a pós colheita, processamento e distribuição, portanto é necessário diminuir os riscos de doenças transmitidas por alimentos contaminados e as embalagens de alimentos podem em muito contribuir para a redução destas contaminações. (8,10).

A embalagem como dito anteriormente, é um meio eficaz de proteção dos produtos alimentícios, principalmente durante seu armazenamento, entretanto os materiais de embalagem convencionais não podem controlar ativamente as reações dentro do produto (10). A ciência e a engenharia de materiais, vêm apresentando novas tecnologias de embalagens, conhecidas como embalagem inteligente/ativa, que auxiliam na manutenção da qualidade e otimiza a segurança do alimento além de aumentar a vida de prateleira (8,10).

Uma das tecnologias de embalagens ativas, consiste na incorporação de agentes antimicrobianos na estrutura polimérica da embalagem, se destacando pela sua eficácia na redução da deterioração de alimentos e na otimização da segurança alimentar (8–12).

Vários tipos de antimicrobianos em polímeros foram estudados e desenvolvidos, em especial aqueles que continham nanopartículas antimicrobianas, com destaque para a prata, com a cadeia polimérica de polietilenos, utilizada em embalagens de alimentos, como pode ser observados pelos trabalhos de Abutalib & Rajeh, Ahmed et al., Becaro et al. e Brito et al. (9,44–46).

Nanotecnologia em Embalagens

Nanopartículas, cuja a escala de dimensão fica na faixa de 1–100 nm, tem como fenômeno o efeito de superfície, ou seja, o aumento da relação área/volume em matérias nanométricos. A redução do volume em detrimento com o tamanho, favorece o aumento da proporção de átomos na superfície, proporcionando propriedades físicas, químicas e ópticas

superiores quando comparadas com os mesmos materiais em escala macro (47–49).

Materiais em nanoescala, baseados em partículas metálicas ou óxidos de metal, vêm sendo empregados nas matrizes poliméricas para incluir a função antimicrobiana nestas estruturas (43). Dentre as nanopartículas se destaca a prata, a qual nas pesquisas realizadas por Becaro et al. (2015), Brito et al., (2020), Lazić et al. (2018), Roy et al. (2017) e Zhou et al. (2020a), mostrou que ela apresenta um espectro maior de atividade antimicrobiana quando comparado com outras nanopartículas metálicas.

Historicamente a prata é utilizada para a eliminação de bactérias, a fim de evitar infecções causadas por estas, mas quando este metal se encontra no tamanho nano, tem apresentado uma otimização do seu desempenho antimicrobiano (54,55), com isso as nanoestruturas da prata vem sendo aplicadas na medicina, cosmetologia e em alimentos (56).

O mecanismo de ação da prata ainda não foi totalmente elucidado, entretanto as suas propriedades antimicrobianas podem estar relacionadas com a liberação de íons de Ag, sendo estes os responsáveis pelas alterações morfológicas e na permeabilidade da membrana microbiana e danos intracelulares (9,52,57).

Entretanto a nanoescala da prata não é garantia de um eficiente desempenho antimicrobiano, pois isso também depende da uniformidade e dispersão destas nanopartículas (52,55). Nanopartículas de prata, apresentam uma alta tendência de formar aglomerados, devido à instabilidade decorrente da alta área de superfície/volume, portanto para evitar tal ocorrência a prata pode ser sintetizada com um carregador

inorgânico, a qual imobilizará a nanopartícula de prata, controlando o seu tempo de contato com os microrganismos, assim como o controle da taxa de liberação de íons prata (52,56,58).

Como carregadores inorgânicos da prata, é de grande interesse escolher a mais utilizada no mercado que é a nano sílica mesoporosa, um substrato inorgânico, e a nano hidroxiapatita, que é tipo de fosfato de cálcio, pois ambas apresentam características favoráveis como biocompatibilidade, dispersibilidade, estabilidade química e grande área de superfície, além de ser baixo custo de produção e seguro para o consumo humano (9,51–53,56–58).

Em suma este trabalho visa investigar se há diferença na eficácia da ação antimicrobiana dos diferentes carregadores sob as nanopartículas de prata integradas em embalagens alimentícias, além disso verificar se está tecnologia pode ser um mantenedor da qualidade físico-química e microbiológica pós pasteurização da água de coco, estendendo a vida de prateleira principalmente em ambientes a qual as condições de controle de temperatura não são eficazes, adicionalmente proporcionando a manutenção da qualidade microbiológica e físico-química por um período maior após o produto ser aberto para consumo

Objetivos

Objetivo Geral

Realizar o processamento de filmes PEBDL contendo AgNPs com carregador de sílica (SiO_2) e hidroxiapatita (HAP) em diferentes concentrações e investigar a eficácia antimicrobiana deste por meio de testes *in vitro* dos e observar a eficiência dos filmes em embalagem para produtos alimentícios na manutenção da qualidade e potencial de extensão da vida de prateleira.

Objetivos Específicos

- Processar por meio de extrusoras filmes de PBDL controle e com os compósitos AgNPs + SiO_2 e AgNPs + HAP;

- Caracterizar aditivos AgNPs + SiO_2 e AgNPs + HAP, e filmes PEBDL sem e com AgNPs + carregadores (SiO_2 e HAP) em diferentes concentrações, por meio da Difração de Raios X, Espectroscopia no Infravermelho com Transformada de Fourier, Microscopia Eletrônica de Varredura, Espalhamento Dinâmico de Luz, Potencial Zeta, Termogravimétrica e Calorimetria Diferencial de Varredura;

- Analisar a eficácia antimicrobiana *in vitro* de filmes PEBDL em diferentes concentrações de AgNPs + SiO_2 e AgNPs + HAP, por meio da metodologia de atividade antimicrobiana por contato nos microrganismos, Gram positiva *Staphylococcus aureus*, Gram negativa *Escherichia coli* e os

fungos *Penicillium expansum* e *Fusarium solani,* e análise de imagens bacterianas por microscopia eletrônica de varredura, nas bactérias citadas acima;

- Analisar a taxa de migração de AgNPs em simulantes ácido e não ácido;
- Analise de permeabilidade de oxigênio de vapor de água das embalagens controle e nanopartículadas;
- Analise de migração de prata em água de coco;
- Analisar a influência da embalagem com AgNPs + SiO_2 e AgNPs + HAP na vida de prateleira de água de coco, por meio de análises físico-químicas, como: pH, acidez titúlavel, sólidos solúveis, cor, turbidez, compostos fenólicos, atividade antioxidante, açucares redutores e não redutores e minerais;
- Analises microbiológicas, durante o armazenamento refrigerado da água de coco, em psicrotróficos, bolores e leveduras, enterobactérias e *Salmonella* spp.;

Capítulo 1.

Antimicrobial potential of linear low-density polyethylene food packages with Ag nanoparticles in different carriers (Silica and Hydroxyapatite)

Sabrina da Costa Brito[ab]
Vinicius Alex Cano Pereira[cb]
Ana Carolina Figueiredo Prado[db]
Thais Juliana Tobias[e]
Elaine Cristina Paris[bf]
Marcos David Ferreira[ba]

[a]Postgraduate Program in Food Science and Engineering, São Paulo State University "Julio de Mesquita Filho", Rod. Araraquara Jaú, Km 01, zip code: 14800-903, Araraquara, SP, Brazil.
[b]Embrapa Instrumentação, Rua XV de Novembro, 1452, zip code: 13560-970, São Carlos - SP, Brazil.

[c]Biotechnology Graduate Program, Federal University of São Carlos, Rod. Washington Luís, Km 235 – C. P.676, zip code: 13.565-905, São Carlos - SP, Brazil.
[d]Postgraduate Program in Materials Science and Engineering, Federal University of São Carlos, Rod. Washington Luís, Km 235 – C. P.676, zip code: 13.565-905, São Carlos - SP, Brazil.
[e]Chemistry Graduate Program, University of Sao Paulo, Av. Trabalhador São-carlense, 400, zip code: 13.560-970, São Carlos - SP, Brazil.
[f]Postgraduate Program in Chemistry, Federal University of São Carlos, Rod. Washington Luís, Km 235 – C. P.676, zip code: 13.565-905, São Carlos - SP, Brazil.

Abstract

This study intended to verify the antimicrobial efficacy of linear low-density polyethylene films incorporated with silver nanoparticles dispersed in silica (SiO_2) and hydroxyapatite (HAP) carriers at different concentrations. The silver nanoparticles showed in most concentrations, an inhibition percentage bigger than 90% in all microorganisms studied, regardless of the carrier. However, a superior inhibitory action on *S. aureus* and between carriers was found, and hydroxyapatite was more effective. The results indicate that the nanostructured films with AgNPs + hydroxyapatite demonstrated promising antimicrobial action against the microorganisms investigated than AgNPs + silica, being the hydroxyapatite with silver nanoparticle a potential for use in food packaging, for enhancing safety and quality maintenance of these products.

Keywords: active food packaging; antimicrobial; inorganic carrier; nanotechnology; polymer films; silver nanoparticles.

Graphical Abstract

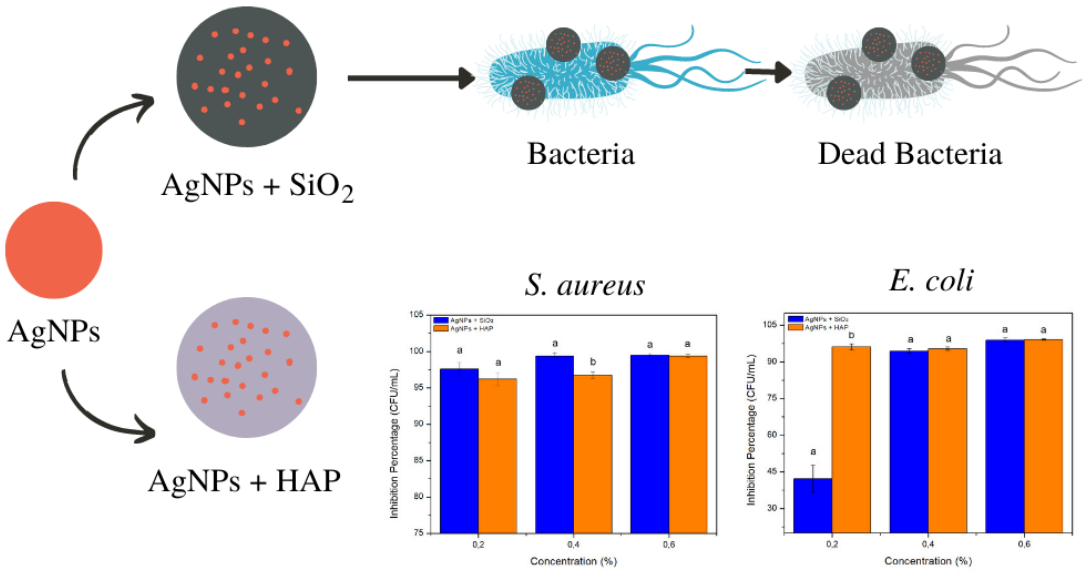

Antimicrobiall Activity

Introduction

Linear low-density polyethylene (LLDPE) is an ethylene copolymer containing a small fraction of α-olefin comonomers incorporated into their polymer chain causing a induction of short chain branching, which can provide improvements in their mechanical properties, such as stiffness, density, hardness, and tensile strength (38–40,59). Furthermore, LLDPE is a thermoplastic commonly used in a wide range of applications due to its superior

processing, abundance, and low cost (Mulla et al., 2017; Panrong et al., 2020; Yaqub et al., 2022) and its application can be both in the preparation of thin film coatings for electronic equipment and additionally in the last decade for production of packaging for food products. The biocidal properties that can be incorporated into these materials have contributed to this progress (40,60–62).

The use of food packaging is essential since it can help reduce the risk of microbiological diseases, as packaging is an efficient way of protecting food products from external microbiological contaminants during their distribution to the final consumer (8,10).

Nanotechnology with antimicrobial agents has become promising in food packaging, mainly due to its more extensive reactivity and high surface area contact, providing the optimization of biological properties when compared to the same materials on a macro scale (60,63–65). A molecular interaction through Van der Waals force and electrostatic attraction occurs when nanoparticles are integrated into the polymeric matrix, allowing free nanoparticles to be transferred from the polymeric medium to the packaging surface, coming into direct contact with the microbial cell membrane inhibiting it. Thus, packaging will contribute to keeping food´s quality and shelf life (10,65). Among the biocidal materials, the most widely used is silver (Ag), due to its broad antimicrobial activity, especially in the form of nanoparticles (9,51,53). Silver nanoparticles (AgNPs) have efficient mechanisms of action against bacteria and fungi, which are related to the interruption of respiratory chain enzymes and DNA replication, in addition to oxidative stress (57,62,66,67).

Research carried out with AgNPs incorporated in polymeric films showed as results an efficient antimicrobial action in the inhibition of microorganisms

such as *Escherichia coli, Listeria monocytogenes, Salmonella Typhimurium, Staphylococcus aureus,* and fungi such as *Penicillium expansum* and *Fusarium solani* (43,55,68,69). The antimicrobial action of silver nanoparticles was also evidenced in biodegradable films from renewable natural resources as starch, corn starch and carboxymethyl cellulose, and in these researches the silver is accompanied by other compounds such as silica, copper oxide, zinc oxide and titanium nanoparticles, showing how this composite manages to combine with various types of materials and maintain its antimicrobial capacity (70–73).

Microbial control is necessary in order to inhibit the proliferation of bacteria and fungi in several industries, especially for food, where contamination can severely impact human health through foodborne illness, caused mainly by bacteria such as *Staphylococcus aureus* and *Escherichia coli* (74–78), as well as accelerate food spoilage by fungi such *as Penicillium expansum* and *Fusarium solani* for example (69,79).

The performance and efficiency of the antimicrobial activity of AgNPs are accomplished when they present uniformity in their size and distribution. However, the small size of the nanoparticles has a high tendency to aggregate due to their instability, which may lead to a decrease in their antimicrobial activity (52,53). In order to solve this problem, silver nanoparticles have been incorporated with inorganic carriers, such as silica (SiO_2) and hydroxyapatite (HAP), which provide the immobilization of AgNPs in their pores, thus reducing the formation of aggregates and enabling efficient nanoparticle´s biocidal action (51–53,56–58).

Properties of mesoporous silica, such as control of particle size, porosity, morphology, and high chemical stability, make it attractive as a silver

nanoparticle carrier. In addition, it presents rapid internalization by animal and plant cells without causing cytotoxicity in the body (80,81). Due to these characteristics in foods, silica associated or not with silver, is a constant presence in the preparation of food packages to improve the shelf life of food products (Biswas et al., 2019; Dong et al., 2022; Wu et al., 2019). Regarding the hydroxyapatite, this is considered an important representative biomaterial based on calcium phosphate, a mineral component of human and animal body tissue and teeth. Because of its biocompatibility, biodegradability, and bioactivity, it is widely exploited in pharmaceutical, agriculture (fertilizer), and biomedical applications, especially when combined (carrier) with silver nanoparticles (51,53,85–88).

The present work aimed to investigate the efficiency of inhibiting the growth of microorganisms, under the presence of AgNPs nanoparticles with two types of carriers, SiO_2 and HAP, which have been incorporated into the matrix of LLDPE films, at different concentrations. This research intent to show the reduce of microbial contaminants through packaging for the food and biomedical areas.

2. Materials and Methods

2.1. Materials

The powder composite of AgNPs with SiO_2 carrier (AgNPs + SiO_2) was obtained from Nanox Tecnologia S.A., a nanotechnology company based in São Paulo, Brazil. The powder composite of AgNPs + HAP was synthesized in the laboratory. The LLDPE masterbatches with AgNPs + carrier and the LLDPE

films control and with nanoparticles were processed by extrusion (APV - Baker & Perkins).

2.2. Hydroxyapatite (HAP) Synthesis

The synthesis of HAP was obtained by wet coprecipitation. First, a solution of 2.8 g of Calcium Nitrate Tetra hydrate (Ca $(NO_3)2._4H2O$) in 43 mL of deionized water was prepared, where after being completely solubilized, it was transferred to a three-neck flask to bubble the nitrogen (N_2) solution. Simultaneously, a solution of 1.6 g of Diammonium hydrogen phosphate ($(NH_4)_2HPO_4$) in 20 mL of deionized water was prepared. The pH of the first solution was adjusted to 11 with the addition of ammonium hydroxide (NH_4OH). Then the $(NH_4)_2HPO_4$ solution was poured into Ca $(NO_3)2.4H_2O$ solution under constant stirring and at room temperature. The precipitate formed was centrifuged at 12,000 rpm for 10 minutes and washed with distilled water until neutral pH was reached. Finally, the product was resuspended in ethanol and dried in an oven with air circulation (89).

2.3. Synthesis of Silver Nanoparticles in HAP

AgNPs were synthesized through precipitation, silver nitrate as a precursor, sodium citrate as a reducing agent, and HAP as a nanocarrier. Initially, a solution of 100 mL of sodium citrate with a concentration of 5 mg/mL was made; then, it was solubilized and kept stirring with heating until it began to boil. After that, 0.54 g of HAP was added and homogenized, and then 0.08 g of silver nitrate was added, where it was left under stirring for one minute, finishing the procedure. In the end, the solution was centrifuged (at 8000 rpm for 1

minute), then the supernatant was discarded, and the solution was resuspended in distilled water. Finally, the solution was lyophilized.

2.4. Preparation of Nanostructured Films

In order to obtain the material in film format, the LLDPE masterbatches with AgNPs + carrier were processed in a single-screw extruder (AX plastics) with heating zones 1, 2, and 3 at 190, 180, and 170 °C, respectively, with a processing speed of 45 rpm/min (59). The films obtained showed the following percentages: 0.2, 0.4, and 0.6 % of $AgNP_S$ + carrier (SiO_2 or HAP), in addition to the LDPE control film without composites.

2.5. Characterization of AgNPs + SiO_2 and AgNPs + HAP Composites and Films

The following characterization procedures were performed for both the AgNPs + carrier composites (SiO_2 + HAP) and the LLDPE films (control and nanoparticulated): X-ray diffraction (XRD) to determine the atomic structure of the materials, using a Shimadzu XRD 6000 30 kV diffractometer, 30 mA current, scanning speed of 1° per minute, and 2θ ranging between 4 and 50°. The FTIR spectrometer (Bruker, model Vertex 70) was applied to detect vibrational frequencies of the sample components at wavenumbers ranging from 4,000 - 400 cm^{-1} in the reflectance mode. Field emission gun analysis (FEG-SEM) in a JEOL 6701F JMS microscope, operating at accelerating voltages from 2 to 10 kV, was employed to verify the morphology and distribution of the nanoparticles in the AgNPs + SiO_2 and AgNPs + HAP composites, as well as in the films (surface and nitrogen fracture).

The dynamic light scattering (DLS) (Malvern Instruments) was performed only for AgNPs + SiO_2, and AgNPs + HAP powder composites to evaluate the dimensions of the particles in suspension at a temperature of 25 °C, a counting rate of 453.3 kcps, and a measurement position of 1.05 mm, as well as the zeta potential in the Malvern Instruments - Zetasizer Nano ZS90 equipment, to check the stability of the dispersion of the particles.

The following analyses were performed on the nanostructured and control films: a thermo gravimetric analyzer TGA Q 500 (TA Instruments) was used to investigate the films' thermal stability at the heating rate parameters of 10 °C/min and range between 10 and 800 °C. The nitrogen and synthetic airflow rates were maintained at 40 mL/min and 60 mL/min, respectively. In addition, to identify the endothermic and exothermic events during heating, Differential Scanning Calorimeter (DSC) DSC Q 100 (TA - Instruments) analysis was performed. Tests were carried out at temperatures between 10 and 200 °C, at a heating rate of 10°/min, and nitrogen flow was maintained at 60 mL/min.

2.6. Microbiological Analysis in Films

The microbial analyses performed in this work were agar-well diffusion (90), antimicrobial activity by direct contact test (91,92), and bacterial imaging by scanning electron microscopy (SEM) (93). The antimicrobial activity by contact was performed on Gram-positive bacteria *Staphylococcus aureus* (INCQS 15 ATCC 25923) and on Gram-negative *Escherichia coli* (INCQS 33 ATCC 25922), as well as on the fungi *Penicillium expansum* (PEN001) and *Fusarium solani* (IMI 314228 CCT 2876). All procedures were performed in triplicate.

2.6.1. Agar-well diffusion

This methodology was performed to evaluate the antimicrobial effectiveness of the concentrations of the composites AgNPs + SiO_2 and AgNPs + HAP that would be added in LLDPE. In a solution containing 10 mL of deionized water, the composites were added separately at concentrations of 0.04, 0.2, 0.4, 0.6, and 0.8 % and then kept in an ultrasonic bath for 15 minutes for particle dispersion. (90).

S. aureus and *E. coli* bacteria were inoculated into 10 mL of tryptic soy broth (TSB) (Kasvi) and incubated at 37 °C for 24 hours. They were adjusted to a concentration of 108 CFU/mL at 625 nm by Ultraviolet-Visible Spectroscopy (UV-VIS) (Shimadzu UV 1650) (90).

Subsequently, a 100-µL aliquot of inoculum was spread onto Mueller Hinton agar (Kasvi) with a Drigalski spatula. With a 100 µL dispenser tip, 5 wells were made on the agar, into which 40 µL of each concentration were pipetted. The plates were incubated at 30°C/24h. The results were quantified by measuring the halo (90).

2.6.2. Direct contact antimicrobial assay

For the direct contact antimicrobial activity assay, stock colonies of *S. aureus* and *E. coli* were grown on tryptic soy agar (TSA) (Kasvi), and one of these colonies was inoculated into 10 mL of tryptic soy broth (TSB) (Kasvi) medium and incubated at 37 °C for 24 hours. After this period, the bacteria were centrifuged (Hettich zentrifugen Routine-390) for 5 minutes at 10 °C and 2000 rpm, the supernatant was discarded, and then the cells were resuspended in

0.9% phosphate-buffered saline solution. Each microorganism inoculum was adjusted by absorbance reading at 625 nm by Ultraviolet-Visible Spectroscopy (UV-VIS) (Shimadzu UV 1650) to the concentration of 10^5 CFU/mL in phosphate-buffered saline solution (Pagno et al., 2015).

As for *Penicillium expansum* and *Fusarium solani*, from the stock culture grown in potato dextrose agar (PDA), for 6 days (at 25 °C), suspensions were prepared to remove further spores by adding phosphate-buffered saline solution with Tween 80 (0.1% v/v) and scraping them with a Drigalski spatula. An aliquot of this suspension solution was used to establish its concentration using the Neubauer chamber (Kasvi) at 10^6 in phosphate-buffered saline solution (Avila-Sosa et al., 2010).

Both control and AgNPs-containing films were shaped into (4 cm x 4 cm) 16 cm^2 squares, disinfected by immersing them in 70 % ethyl alcohol for 15 minutes, and accommodated in the inner wall of Eppendorf tubes. Then 500 µL of microbial suspension was added and incubated under gentle shaking in the rotary incubator (100 rpm) for 24 hours at room temperature (±25 °C) (Pagno et al., 2015).

Subsequently, a 100 µL aliquot of the microbial suspension (bacteria and fungus) was taken from each tube and transferred to an Eppendorf containing 900 µL of phosphate-buffered saline solution to then obtain serial dilutions, where each dilution was vigorously homogenized with the aid of a vortex (Pagno et al., 2015).

In both bacteria, 10 µL of the microbial solution of each dilution were seeded in drops on tryptic soy agar (TSA) and incubated at 37 °C for 24 h. Regarding *Penicillium expansum* and *Fusarium solani*, each dilution was

transferred to a Neubauer chamber (Kasvi), where germinated and non-germinated conidia were counted (91,94).

In bacteria, the number of colony-forming units was multiplied by the inverse of the dilution to be later analyzed by percentage reduction. In the fungus, a percentage ratio of germinated and non-germinated conidia was performed, all with a confidence interval of 95% (95).

2.6.3. Bacterial Images by Scanning Electron Microscopy (SEM)

To observe the antimicrobial action of nanostructured films against Gram-positive *Staphylococcus aureus* (10^7) and Gram-negative *Escherichia coli* (10^6), a JSM-6510/JEOL scanning electron microscopy (SEM) was used, where the bacteria were initially submitted to the contact antimicrobial activity procedure, without undergoing serial dilutions. Then 10 µL of the bacterial solution were placed in the center of slides previously treated with a dispersion of 0.1 % poly-L-lysine solution. Next, the slides were placed inside Eppendorfs tubes and filled with Karnawesk solution for 4 hours, after which the samples were washed with cacodylate buffer and distilled water and dehydrated with 30% acetone (10 min), 50% (10 min), 70 % (10 min), 90 % (10 min) and 100 % (three times for 10 min). Next, the samples were lyophilized (Liotop L 101), following the manufacturer's instructions, for 24 hours and then kept in a desiccator until they were fixed in stubs and coated with gold. (93).

2.7. Silver Migration

The evaluation of AgNPs migration of LLDPE films was based on the technical regulation of the Collegiate Directorate Resolution - RDC n° 51/2010 and the European Union Standard EN 1186-1:2002. A 100 cm^2 of control and nanostructured specimens were immersed in 100 mL of simulant A (aqueous non-acidic food simulant (pH > 4. 5): distilled water) and simulant B (aqueous acidic food simulant (pH < 4.5): 3 % (m/V) acetic acid solution in distilled water). The samples were stored in an incubator at 20 °C for 10 days (Brazil - Ministry of Health, 2010; Standards, 2002). After this period, silver was quantified using a flame Atomic Absorption Spectrometer PinAAcle 900T (Perkin Elmer) at a wavelength of 328.07 nm, a spectral band of 0.7 nm, and an oven program in the following parameters: drying 1, 90°C, drying 2, 120°C, pyrolysis, 800°C and atomizing at 1600°C. The argon flow rate during the procedures was 250 mL/min.

Statistical Analysis

For the microbiological results, the statistical analysis was performed by the mean and standard deviation of the logarithmic reduction, with a confidence interval of 95%. For the migration results, it was performed the analysis of variance (ANOVA) and Duncan's multiple range test; the statistical procedures were conducted using the R software version 3.3.3 at a significance level of 5%.

3. Results and Discussion

3.1. Characterization

In XRD, the composites and the films were characterized according to the order in a medium and long distance of the crystal lattice by X-ray diffraction

(Figures 1 and 2). Initially, it was possible to observe that all nanoparticles presented typical peaks of their pure crystalline structures. For Ag nanoparticles immobilized on the silica surface, peaks were observed in 2θ at 38.23° (111) belonging to the silver plane according to ICSD standard #604631 for metallic silver (Figure 1) (52,96). In addition, a broad peak at 22.32° (2θ) according to JCPS file 29-0085 characteristic of silica in its amorphous phase was also verified. In short, the presence of both components was found, indicating the efficiency of silver synthesizing on the silica surface (97,98).

Regarding hydroxyapatite, preferential peaks in 2θ were observed at 26.01° (002), 32.12° (211), and 33.20° (112), indicating a good crystallization of the hexagonal structure of hydroxyapatite, according to ICSD standard #26204 (40,89,96). In addition, silver was detected in a small peak at 44.2° (200) (Labanni et al., 2020; Anasuya Roy et al., 2017), confirming the efficiency of synthesizing silver on the hydroxyapatite surface.

The presence of mesoporous silica and hydroxyapatite, as nanocarriers of silver, is essential since they, as inorganic carriers, present advantageous characteristics of biocompatibility, dispersibility in solution, and chemical stability, which provides the immobilization of AgNPs in their pores, thus helping to reduce the formation of aggregates that reflects in the increase of the antimicrobial performance (52,53,56–58).

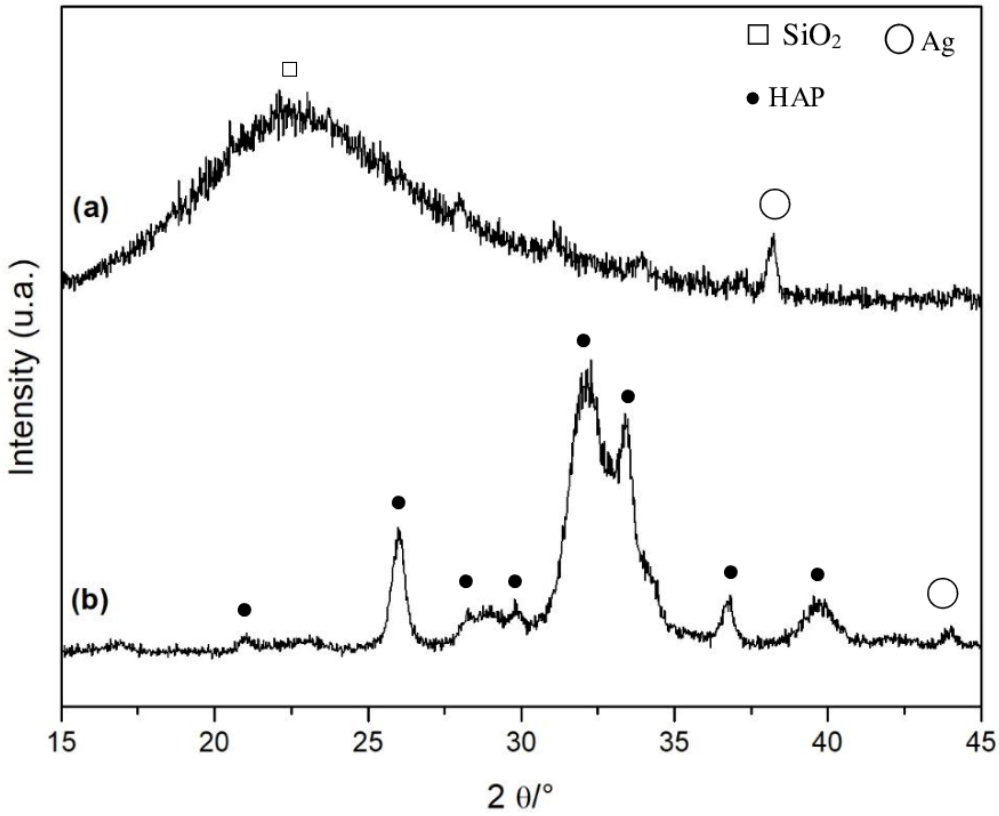

Fig. 1. Intensity in arbitrary unit (a.u.) versus the diffraction angle 2θ/° of (a) silica and (b) hydroxyapatite.

Concerning the control and nanostructured films, peaks in 2θ were presented at 21.40° (110), 23.7° (200), and 36.2° (020), corroborating the polyethylene orthorhombic crystal structure, in line with the specific crystallographic planes (Miller index) (Figure 2) (43,99–101).

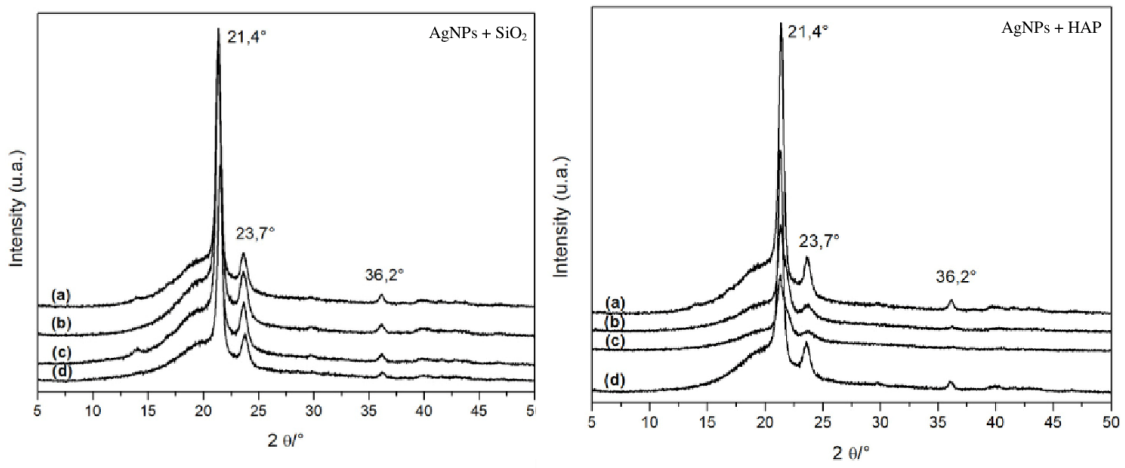

Fig. 2. Intensity in arbitrary unit (a.u) versus the diffraction angle 2θ/° of control and nanostructured samples: (a) control, (b) 0.2%, (c) 0.4% and (d) 0.6%.

As shown in Fig. 2, only polyethylene diffraction peaks are present in the analyzed samples. This fact may be due to the concentration of the composites being much lower than the concentration of LLDPE and consequently masking the peaks of the composites, corroborating the results obtained by Becaro et al. (2015) and Brito et al. (2019). They also did not detect the presence of Ag and carriers in their polymeric films.

In order to confirm the structural characteristics of the composites and films and the absence of impurities, FTIR analysis was performed (Figures 3 and 4). For AgNPs + SiO_2 (Figure 3), it was observed the vibrational mode of silica located at 456 cm^{-1} referring to the Si-O-Si bond, 1072 and 802 cm^{-1} related to the tetragonal Si-O bond, and the band observed in 960 cm^{-1} corresponds to the presence of Si-OH groups (102,103). Regarding AgNPs + HAP (Figure 3), the bands present at 470, 557, 604, and 1028 cm^{-1} are related to the angular vibration of the phosphate group, and the bands 965 and 1421 cm^{-1} are related to the vibrational stretching of the phosphate and the presence of the carbonate group respectively (53,104,105).

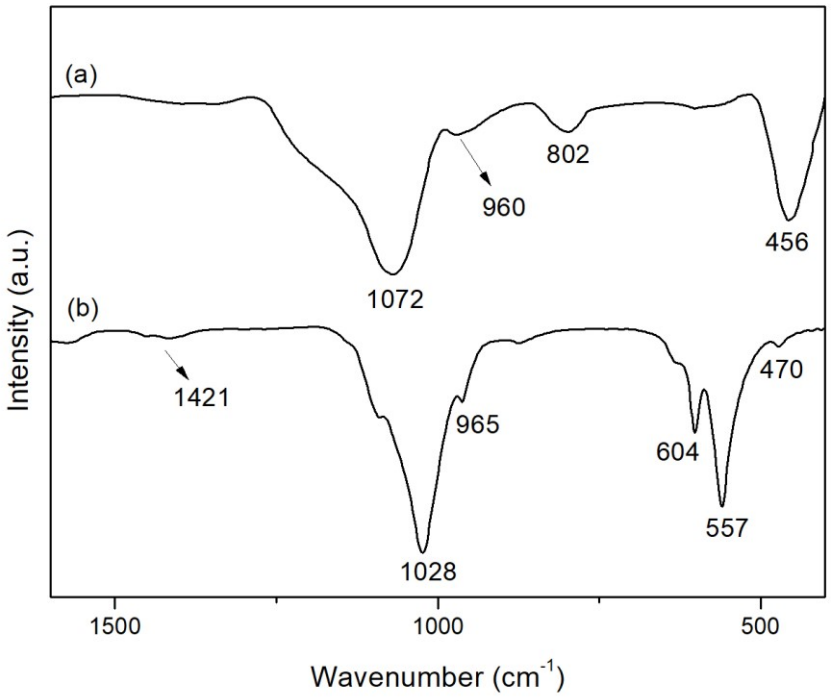

Fig. 3. Transmittance versus wavenumber/cm-1 of (a) hydroxyapatite and (b)silica.

Fig. 3 also shows that only the bands of the carriers are present in the composite samples. The absence of Ag in the analysis may be attributed to its low concentration in the sample, below the detection threshold of the equipment.

Concerning the control and nanostructured specimens, it can be verified that they presented bands typical of pure LLDPE. The bands at 2914 - 2849 cm^{-1} correspond to the C-H stretching, 1464 cm^{-1} represents the CH_2 bending, 1367 -717 cm^{-1} coincides with the vibration of the polymer chain CH_2 (Figure 4)(43,106).

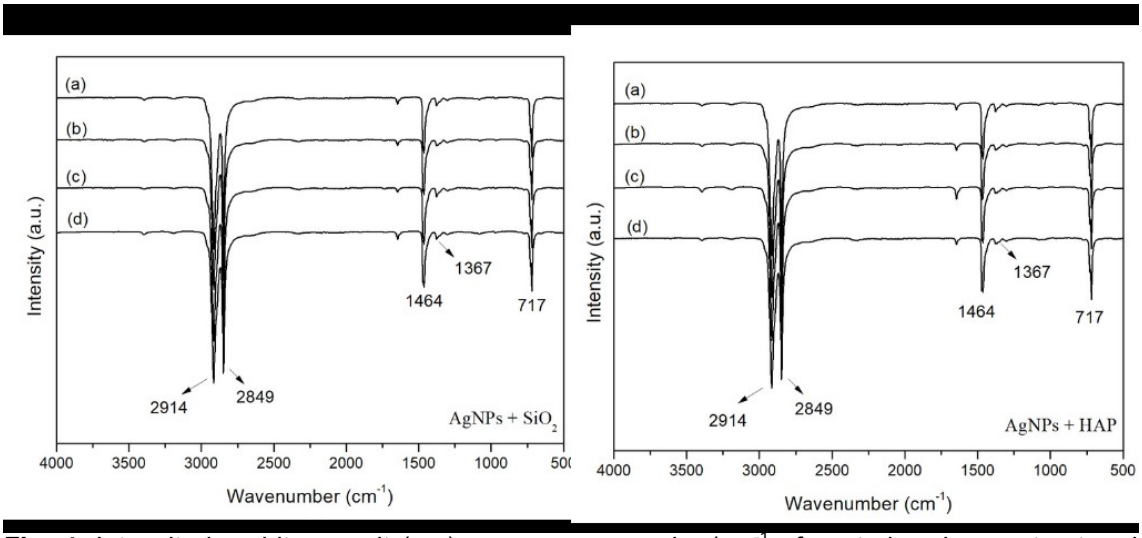

Fig. 4. Intensity in arbitrary unit (a.u) versus wavenumber/cm^{-1} of control and nanostructured samples: (a) control, (b) 0.2%, (c) 0.4% and (d) 0.6%.

Fig. 4 did not show characteristic bands of the composites, and their absence may be due to their concentrations being lower than the LLDPE concentration, consequently masking the composite bands.

The morphology and distribution of AgNPs + SiO2 and AgNPs + HAP particles in the films were verified using FEG-SEM, where the images obtained by the backscattered FEG can observe illuminated particles. The backscattered FEG analysis captures information related to the deepest layers of the samples based on their atomic composition, that is, the AgNPs + SiO_2 and AgNPs + HAP particles. As they have a higher atomic number than the other components of the LLDPE film, a better light contrast is observed in both surface and cross-sectional images (107).

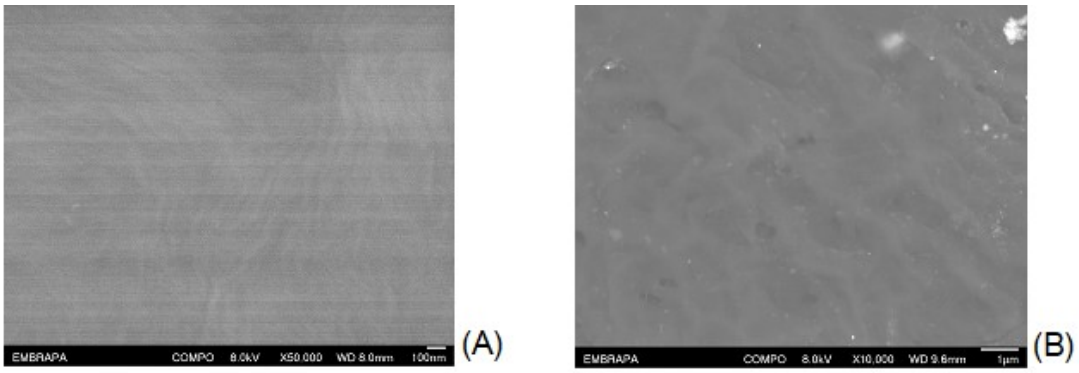

Fig. 5. Surface (A) and cross-sectional (B) images of control LLDPE film.

Based on the atomic composition, contrary to what was observed in the control film (Figure 5), in which illuminated elements were not verified. In Figure 6 is observed light particles dispersed both on the surface and the cross-section of AgNPs + SiO_2 films at concentrations of 0.2, 0.4, and 0.6%, proving their nanostructured form. The same could be observed in the research done by Brito et al. (2019) with LDPE film with Ag nanoparticles with silica carrier. A particle cluster at the 0.6% concentration (Fig. 6 - A) and this agglomeration may be related to the increased concentration of AgNPs in the film. After that, it can be deduced that the silica carrier failed to prevent this agglomeration at high concentrations, similar to what was found in the study by Olmos et al. (2018).

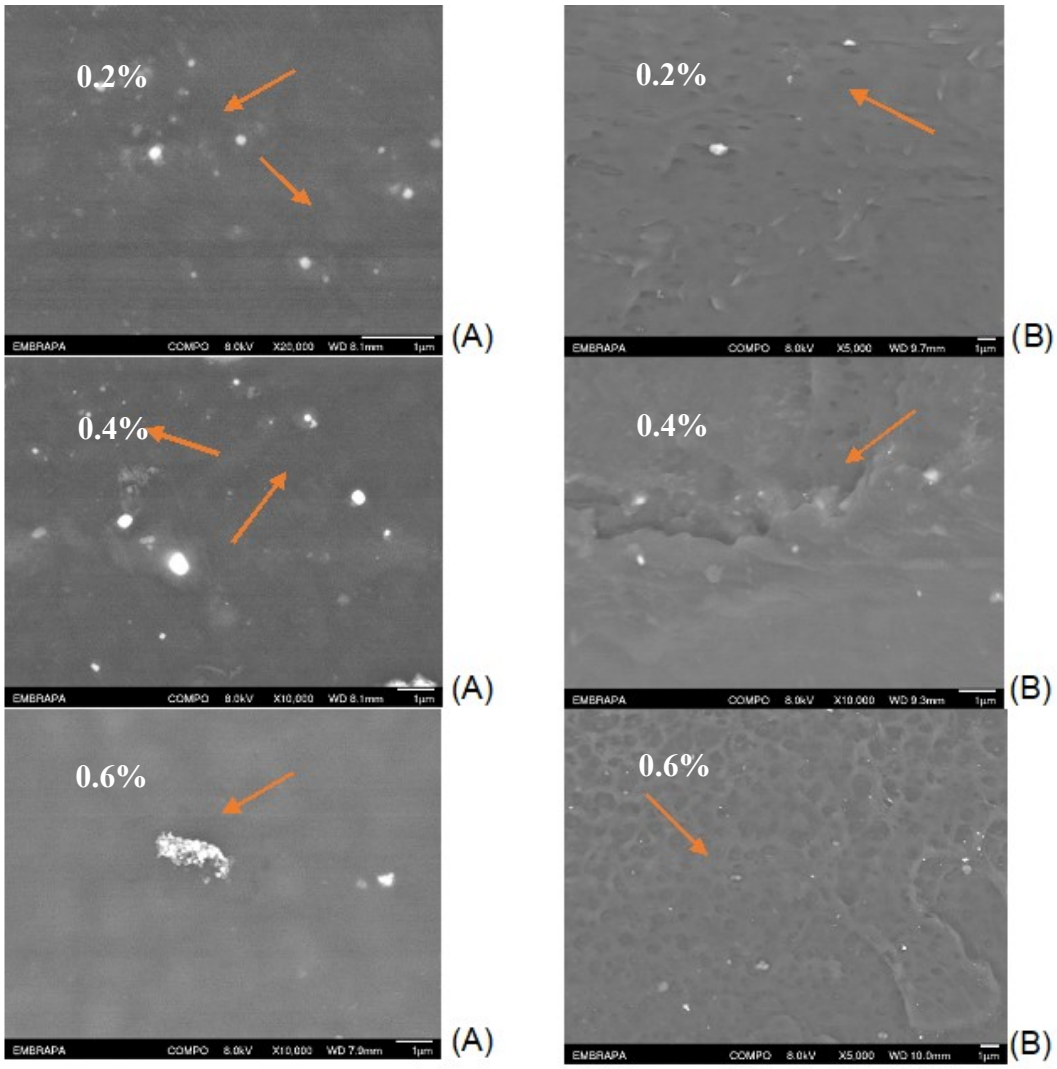

Fig. 6. Surface (A) and cross-sectional (B) images, indicating AgNPs + SiO_2 nanoparticles in LLDPE film.

In the films with AgNPs + HAP at concentrations of 0.2, 0.4, and 0.6%, its nanostructure can also be confirmed through the brighter particles dispersed on the surface and in the cross-sections captured by the backscattered FEG (Figure 7). Furthermore, the presence of small aggregates with increasing concentration of AgNPs, infers that HAP could not avoid agglomerations of silver at high concentrations.

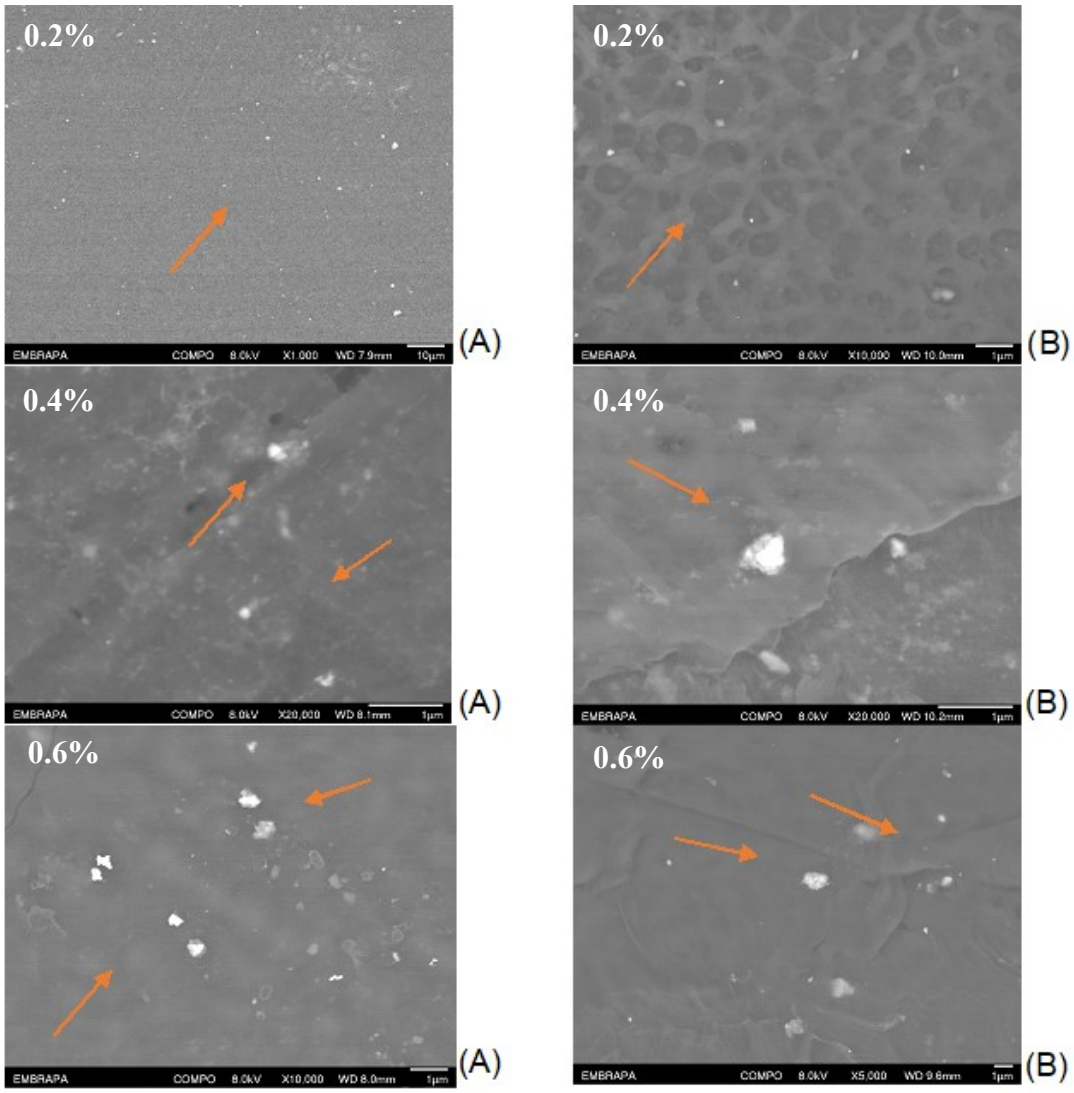

Fig. 7. Surface (A) and cross-sectional (B) images, indicating AgNPs + HAP particles in the nanostructured LLDPE film.

In order to assess the nanoparticle size distribution of the composites, the DLS analysis showed that AgNPs + SiO_2 had an average particle/cluster size of 495.9 nm, while AgNPS + HAP was 280.6 nm (Figure 8). The size of particles/agglomerates is related to the particles' size and homogeneity of dispersion (Pereira et al., 2017; Zhou et al., 2020). Therefore the AgNPs + HAP for having an average particles/agglomerates size smaller than AgNPs + SiO_2; it can be deduced that the synthesis of hydroxyapatite with silver provided smaller particles with greater dispersion homogeneity.

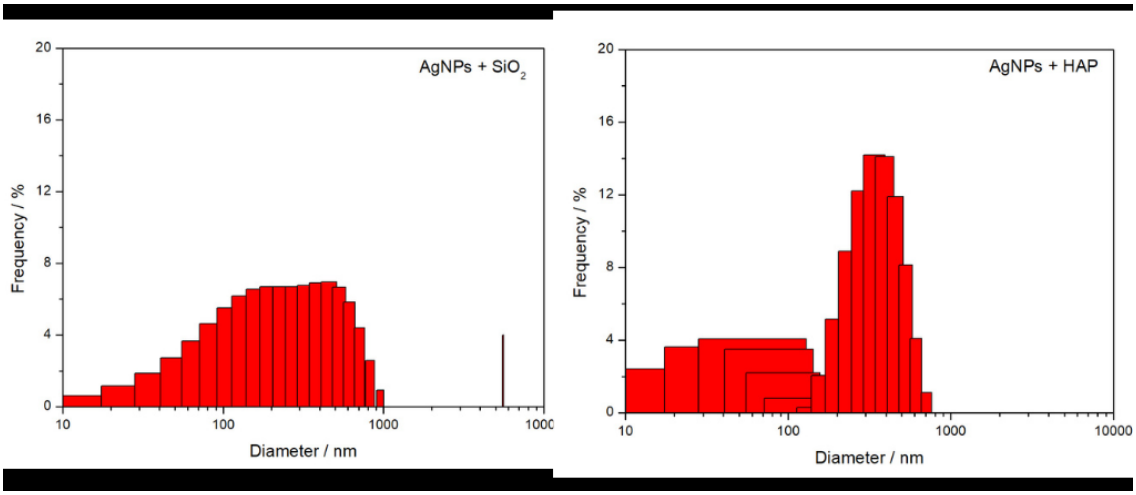

Fig. 8. Intensity versus the size of AgNPs + SiO2 and AgNPs + HAP nanoparticles.

Regarding the stability of the suspensions of the composites AgNPs + SiO_2 and AgNPs + HAP, both presented zeta potential values of 26 mV (Table 1). As particle´s agglomeration is more likely to occur when the zeta is between -30 mV and 30 mV, and the agglomeration speed is increased when it is closer to zero, the analyzed samples, despite presenting an average value lower than 30 mV, are closer to this value and farther from zero, which may indicate less particle agglomeration (Marsalek, 2014).

Table 1
Distribution of zeta potential (mV) data in composites AgNPs + SiO_2 and AgNPs + HAP.

	Silica	**Hydroxyapatite**
Zeta Potential (mV)	26 ± 0.5	26 ± 0.7

In the TGA analysis, both the control and the nanostructured films showed thermal stability similar to that of LLDPE (Fig. 9), as we can observe in the extrapolated onset degradation temperature (T_{onset}) in the TGA analysis curve (Fig. 9). In the Derived analysis curve (DTG) is verified peaks of degradation of polyethylene compounds both in the control and films and of nanoparticles compounds in nanostructured films. In the TGA, we have

observed that the T_{onset} (Table 2) of the control is slightly smaller than that of the films that contain nanoparticles, demonstrating that the presence of metals and inorganic components causes its polymeric structure to present heterogeneity and thus increasing its degradation temperature (108–110).

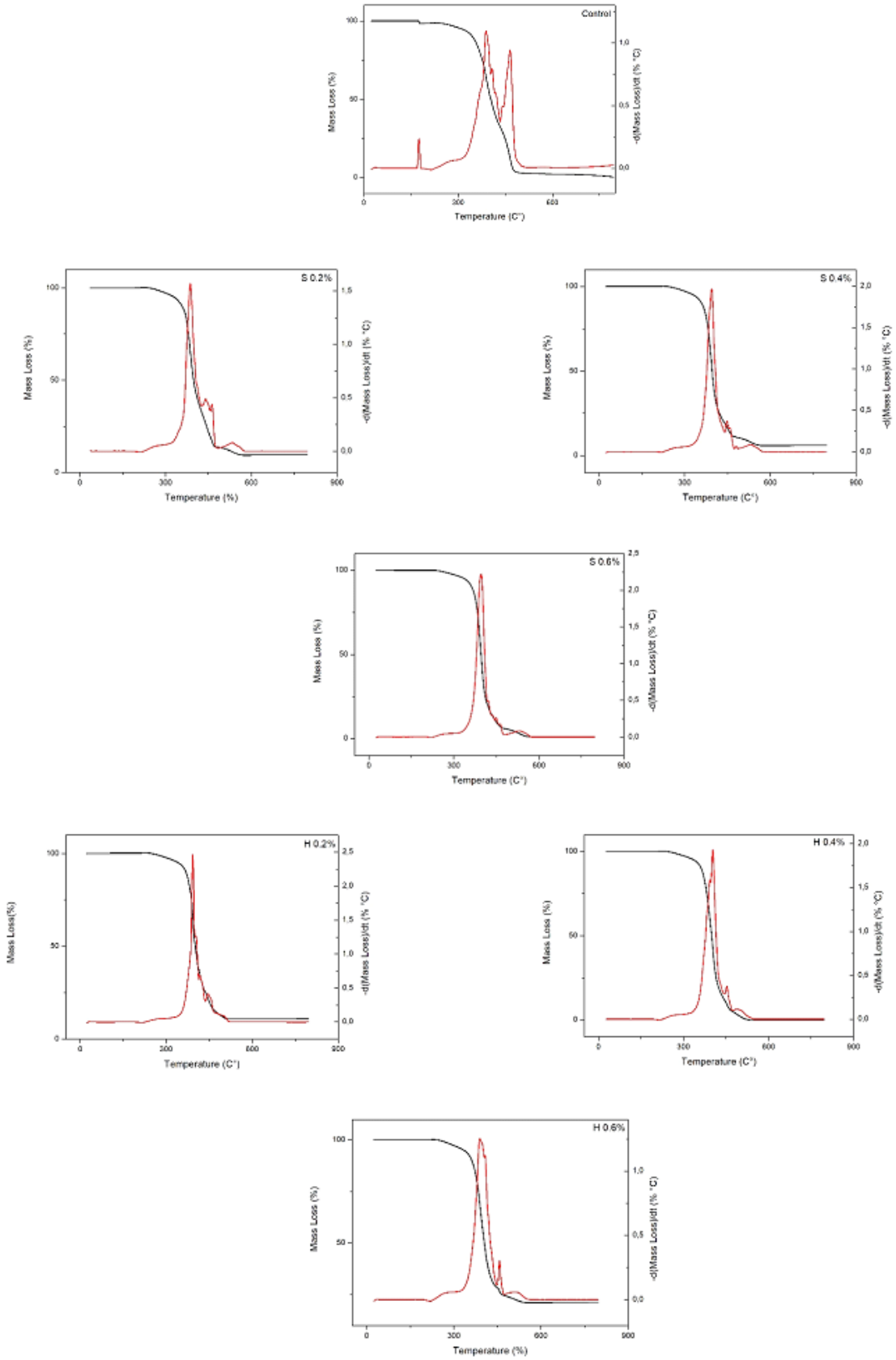

Fig. 9. TGA (black) and DTG (red) curves for control and nanostructured samples, AgNPs + SiO_2 and AgNPs + HAP

Regarding the residual percentage at 700 °C (Table 2), some nanostructured samples showed a higher residual amount than the control LLDPE, suggesting heterogeneity with the polymeric system, thus corroborating the results of T_{onset} (50).

Table 2. Distribution of extrapolated onset degradation temperature (Tonset) and residual percentage at 700 °C (R(%)) of control and nanostructured samples (%).

Concentrations (%)	T_{onset} (°C)	R/700 °C (%)
Control	354.74	99.50
S 0.2	364.15	90.43
S 0.4	370.76	94.04
S 0.6	373.78	98.96
H 0.2	379.39	89.15
H 0.4	373.09	99.20
H 0.6	364.34	78.76

Concerning DSC, it was observed that both the control samples and the nanostructured ones presented a melting temperature (Tm) characteristic of LLDPE (Figure 10) (43,60,99,111,112). The same could be observed by Bumbudsanpharoke et al. (2018) and Brito et al. (2019) that when comparing Tm of pure LDPE films with LDPE plus AgNPs, there was no variation in the melting temperature of the polymeric material when composites were included.

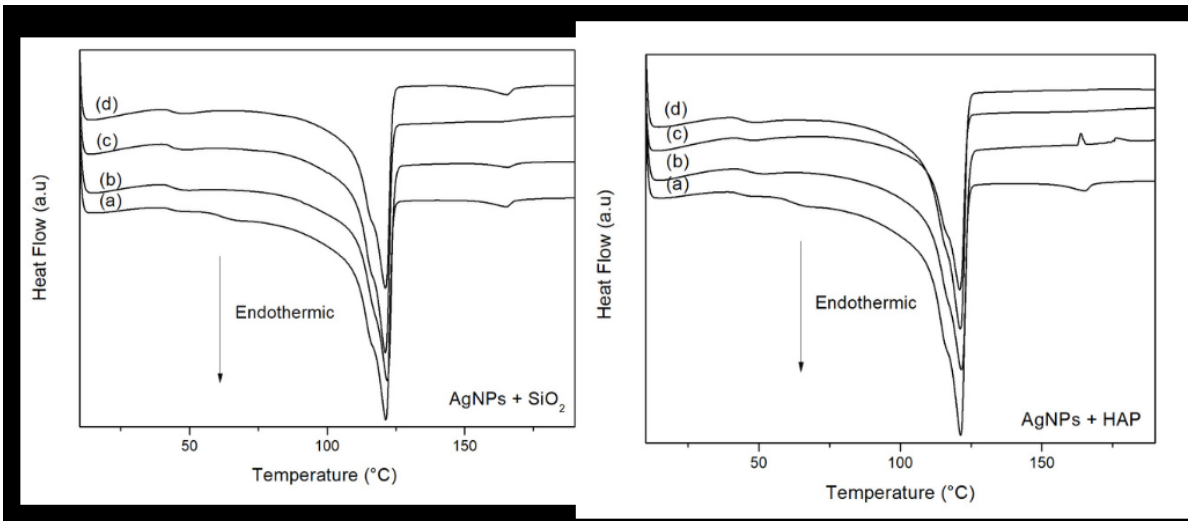

Fig. 10. Differential Scanning Calorimetry (DSC) in control and nanostructured samples: (a) control, (b) 0.2%, (c) 0.4% and (d) 0.6%.

Regarding the melting enthalpy (ΔH), it was observed that there was a variation in the nanostructured samples compared to the control ones (Table 3). This fact may be due to a strong interaction between the masterbatch and the polymer matrix to form a homogeneous distribution, promoting the reduction of the molecule mobility upon heating and thus decreasing the energy absorbed during the process (9,114)

Table 3
Distribution of melting temperature (Tm) and melting enthalpy (ΔH) data of control and nanostructured samples (%).

Concentrations (%)	**T_m (°C)**	**ΔH (J/g^{-1})**
Control	121.30	84.28
S 0.2	121.10	78.06
S 0.4	121.15	79.33
S 0.6	121.81	83.41
H 0.2	121.57	75.16
H 0.4	121.00	76.97
H 0.6	121.11	82.14

3.2. Microbiological evaluations

The antimicrobial efficacy of the concentrations of AgNPs + SiO_2 and AgNPs + HAP composites on LLDPE was evaluated on the agar-well diffusion analysis at concentrations of 0.04, 0.2, 0.4, 0.6, and 0.8 % of composite, where the inhibition was measured through the diameter (cm) of the halo formed. Nanoparticles at both carriers showed inhibitory activity against the tested microorganisms (Figure 11).

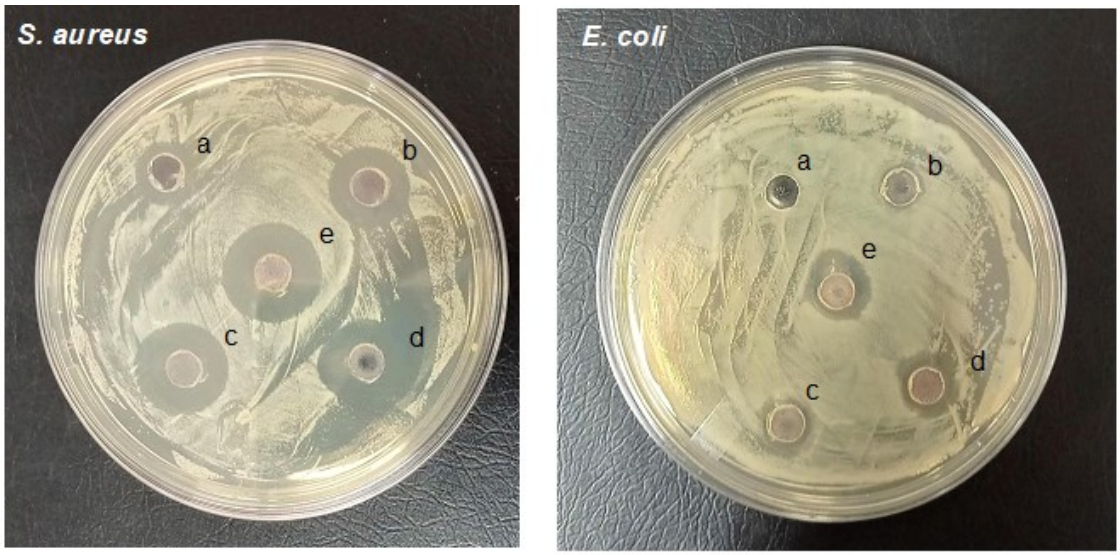

Fig. 11. Inhibition halo formed in contact with the composite AgNPs + SiO_2 and AgNPs + HAP, at concentrations of 0.04% (a), 0.2% (b), 0.4% (c), 0.6% (d) and 0.8% (e), in *S. aureus and E. coli.*

The inhibition halo (cm) was higher in Gram-positive bacteria (*S. aureus*) than in Gram-negative bacteria (*E. coli*) (Figure 11) for both carriers (Table 4). Moreover, we can verify in both bacteria that AgNPs + SiO_2 presented higher inhibition than AgNPs + HAP, and that the higher the concentration, the greater the inhibition of microorganisms. Bacterial inhibition showed statistical differences among concentrations. For *S. aureus,* there was a statistical difference among the concentrations of AgNPs + SiO_2 starting at 0.6% and

hydroxyapatite from 0.2%. *E. coli*, bacterial inhibition statistic differences were found in silica carrier concentrations from 0.2% and for AgNPs+ HAP at 0.4% (Table 4).

Table 4. Mean ± standard deviation data distribution of inhibition halo diameter (cm) in *S. aureus* and *E. coli*, with respect to 0.04, 0.2, 0.4, 0.6, 0.8 % concentration of AgNPs + SiO2 and AgNPs + HAP composites.

	Diameter (cm)	
Concentration (%)	***S. aureus***	***E. coli***
S 0.04	1,100 ± 0.10[a]	0,783 ± 0.07[a]
S 0.2	1,300 ± 0.10[a]	0,967 ± 0.05[b]
S 0.4	2,033 ± 0.17[a]	1,100 ± 0.10[bc]
S 0.6	2,100 ± 0.05[b]	1,467 ±0.15[c]
S 0.8	2,267 ± 0.25[b]	1,167 ± 0.05[d]
H 0.04	1,167 ± 0.20[a]	0,833 ± 0.05[a]
H 0.2	1,500 ± 0.20[b]	0,933 ± 0.05[a]
H 0.4	1,483 ± 0.28[bc]	0,900 ± 0.17[b]
H 0.6	1,567 ± 0.11[bc]	1,233 ± 0.15[b]
H 0.8	2,033 ± 0.15[c]	1,300 ± 0.17[b]

*Mean values followed by the same letter (a, b, c, or d) within the same column do not differ significantly, as indicated by Duncan tests (p>0.05).

Higher resistance to antimicrobials observed in Gram-negative bacteria (*E. coli*) than in Gram-positive bacteria (*S. aureus*) was also detected in other studies with silver nanoparticles (Becaro et al., 2015; Gomaa, 2017; Rahimi et al., 2016), and its related to the differences in structure. Gram-negative bacteria present an outer membrane in the cell wall giving a critical ability to resist antimicrobial agents, unlike the Gram-positive (*S. aureus*), that besides presenting a thicker peptidoglycan layer, do not have this outer membrane (63,115–120).

Based on the statistical results of this analysis, it was established that the study of AgNPs + SiO_2 and AgNPs + HAP incorporated in LLDPE would be conducted at concentrations starting at 0.2, 0.4, and 0.6%.

In order to analyze the antimicrobial activity of polymeric films with silver nanoparticles and verify if there is a difference in inhibition with different

carriers, a direct contact antimicrobial assay was performed, where the percentage of inhibition of these specimens could be measured quantitatively when compared to the control ones for bacteria and fungi. It can be observed by this assay (Figs. 12-15) that nanoparticles with both carriers presented antimicrobial activity against the tested microorganisms. In the case of bacteria, the percentage of inhibition in *S. aureus* was higher than in *E. coli*, similar to what was observed in the agar-well diffusion analysis. Furthermore, the antimicrobial action intensified with increasing AgNPs concentration on all microorganisms; this was observed in both carriers.

For *S. aureus* (Figure 12), it was possible to observe a bacterial inhibition higher than 90% in all concentrations and carriers, showing a positive correlation between concentration and inhibition. Only for the concentration of 0.4%, a statistically significant reduction of the bacterial population in films with AgNPs + SiO_2 compared to AgNPs+ HAP films, 99.38 % SiO_2 and 96.74 % HAP, respectively.

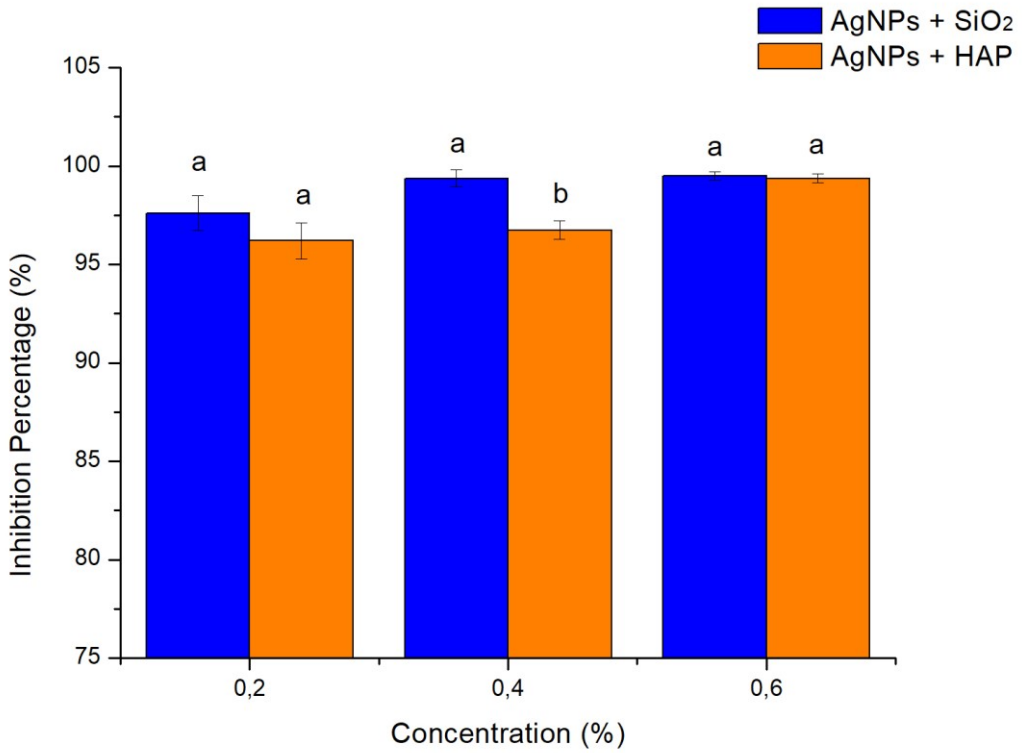

Fig. 12. Inhibition percentage results of *S. aureus* to LLDPE with AgNPs + SiO_2 and AgNPs + HAP.

In turn, for *E. coli* (Figure 13), unlike *S. aureus*, hydroxyapatite significantly reduced the bacterial population, with a statistical difference with silica at the 0.2 % concentration (42.23 % SiO_2 and 96.54 % HAP). For the other concentrations (0.4 and 0.6%), there were no statistical differences between carriers and bacterial inhibition higher than 90%.

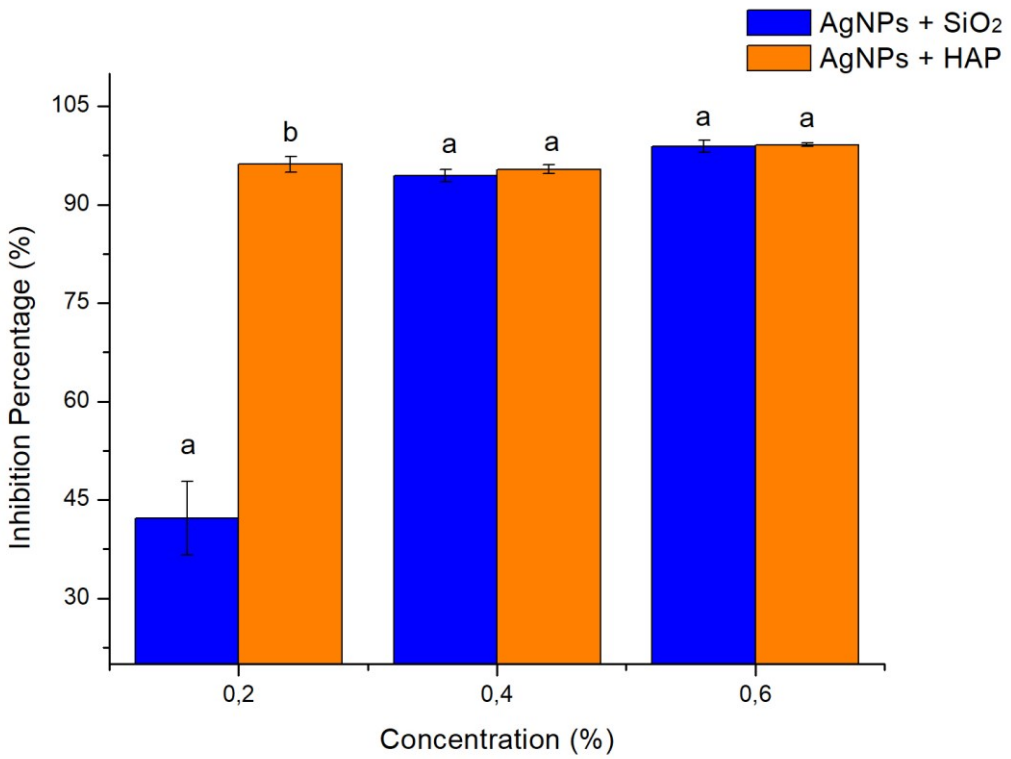

Fig. 13. Inhibition percentage results of *E. coli* to LLDPE with AgNPs + SiO_2 and AgNPs + HAP.

.

This analysis also verified a lower inhibition of antimicrobials in the Gram-negative bacteria (E. coli) compared to Gram-positive bacteria (P. expansum). However, as previously mentioned, this result may be related to the differences in the structure besides that Gram-negative bacteria may present a lower sensitivity to reactive oxygen species (ROS) when compared to Gram-positive bacteria (Liang et al., 2012; Moniri Javadhesari et al., 2019; Padmavathy & Vijayaraghavan, 2008; Rahimi et al., 2016; Russell, 2003; Sondi & Salopek-Sondi, 2004; Yamamoto, 2001).

In the fungi studied, *P. expansum*, AgNPs + HAP showed a higher significant inhibition in the films at 0.2% compared to AgNPs + SiO_2 (Figure 14). For the other concentrations, similar results were found with 90% of inhibition for both carriers. Similar results were found in the case of F. solani, with a more

significant reduction of germinated conidia observed in the AgNPs + HAP films at 0.2% concentration (Figure 15).

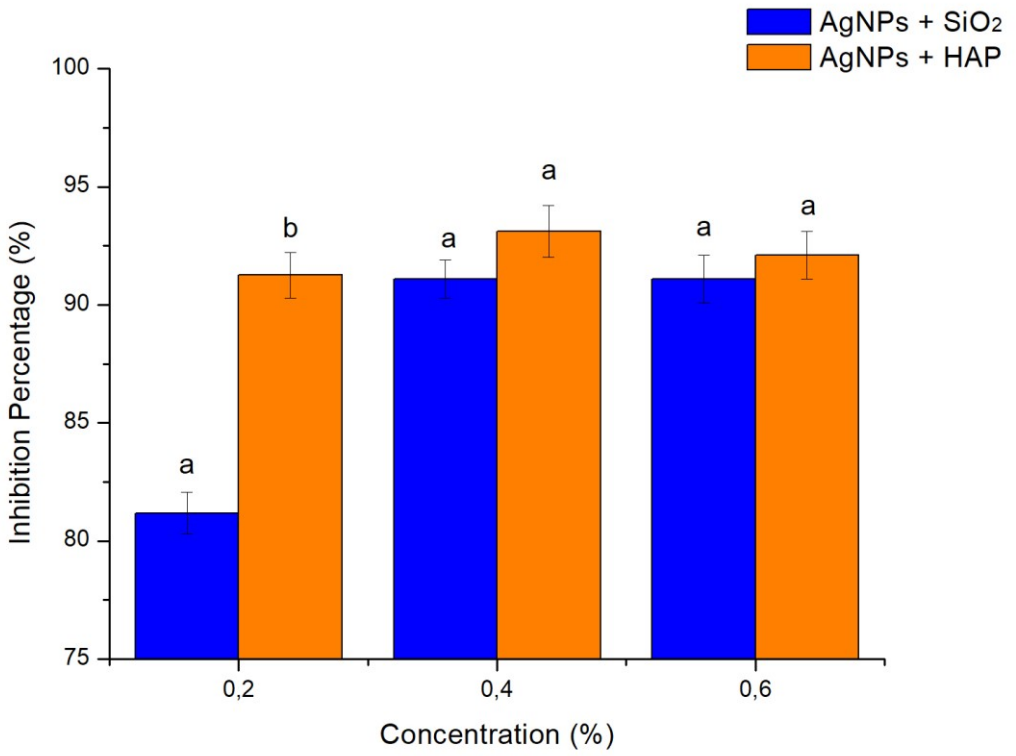

Fig. 14. Inhibition percentage results of *Penicillium expansum* to LLDPE with AgNPs + SiO_2 and AgNPs + HAP.

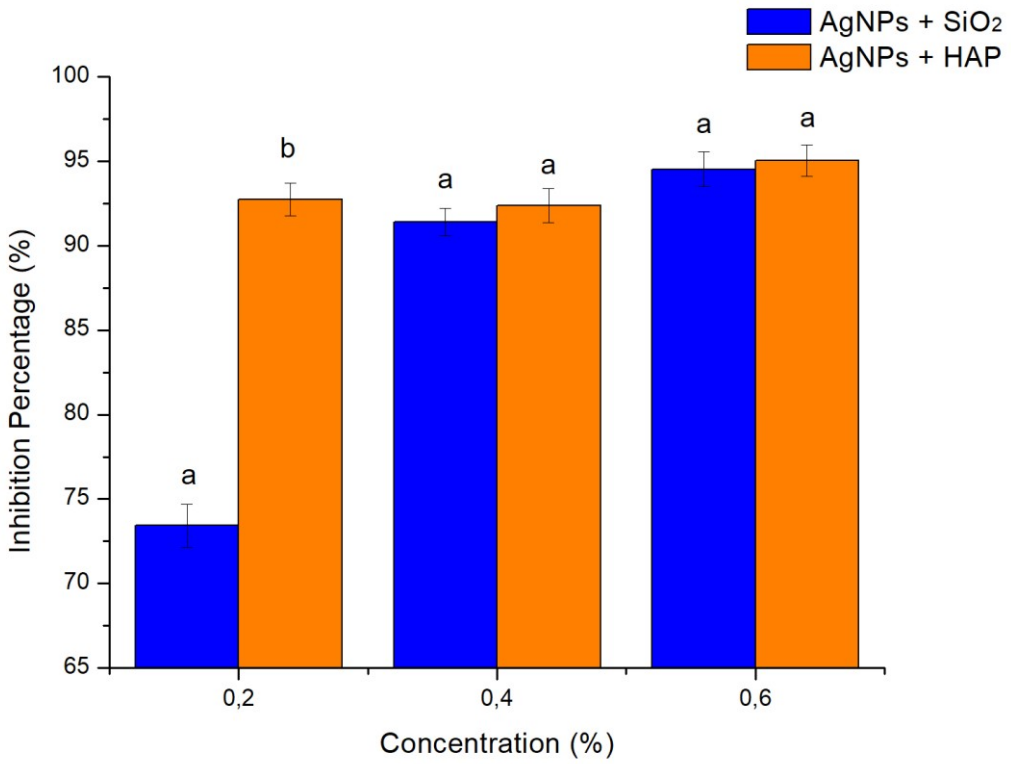

Fig. 15. Inhibition percentage results of *Fusarium solani* to LLDPE with AgNPs + SiO_2 and AgNPs + HAP.

It has been reported that fungi showed lower inhibition percentages than bacteria (Matei et al., 2021). However, in most concentrations studied, there was an inhibition of conidia bigger than 90%, except 0.2% concentration of AgNPs + SiO_2, demonstrating an efficient fungal inhibition. That corroborates the results of other research where inhibition of both fungi by silver nanoparticles was also observed (79,121–125).

The antimicrobial mechanisms of action of AgNPs, although not well elucidated, may be associated with the cell wall and membrane damage, intracellular damage, and an increase in ROS (53,69,79,124,126).

The first contact between nanoparticles and microorganisms is their adhesion to the microbial cell wall and membrane. This interaction occurs by electrostatic attraction since the microbial cell is negatively charged, and the

silver nanoparticles contain a positive charge (126–128). After this interaction, AgNPs induce morphological changes in the membrane. In the case of fungi, besides affecting the membrane, the silver nanoparticles deform the structures of the mycelia and conidiophores (69,79,126–128). Changes in structures lead to a disorder of permeability and respiratory functions due to membrane depolarization, which can lead to cell death. Nanoparticles also damage the microbial wall, allowing them to enter the cell and thus interact with DNA and enzymes (126–128).

Concerning DNA, the silver ions cause it to go from a relaxed to a condensed state, thus losing its ability to replicate. In addition, the ions interact with enzymes that act mainly in the respiratory chain through proteins of the thiol groups (126,129).

ROS molecules present oxygen with a strong redox potential, which under normal conditions results in a balanced production and antioxidant capacity in the cell. Though ROS molecules are exposed to AgNPs ions, there is an imbalance in their antioxidant capacity and the increased production of ROS, which causes redox to favor oxidation, leading to oxidative stress, which consequently leads cells to have protective responses of defense mechanisms. However, when oxidative stress overcomes the defense mechanisms, free ROS damages the cell wall and biomolecules such as proteins, lipids, and DNA (69,79,126,128).

In this analysis, it can be verified that for *E. coli, P. expansum, and F. solani*, the inhibitory action was more effective in the AgNPs + HAP carrier in all concentrations. This fact may be because this composite has a smaller size than the other, as could be observed in the DLS analyses. Thus, facilitating its

diffusion and entry into the microbial cells, and also due to the increase of its surface area that provides a better immobilization of AgNPs, therefore optimizing its antimicrobial performance in the long term (51–53,56–58,68,105).

Regarding the bacterial images performed by SEM, we can observe in Figures 16 and 17 that the microorganisms, when in contact with the AgNPs present in the films in both carriers, showed changes in the structure of their cell wall in all concentrations, starting on 0,2%.

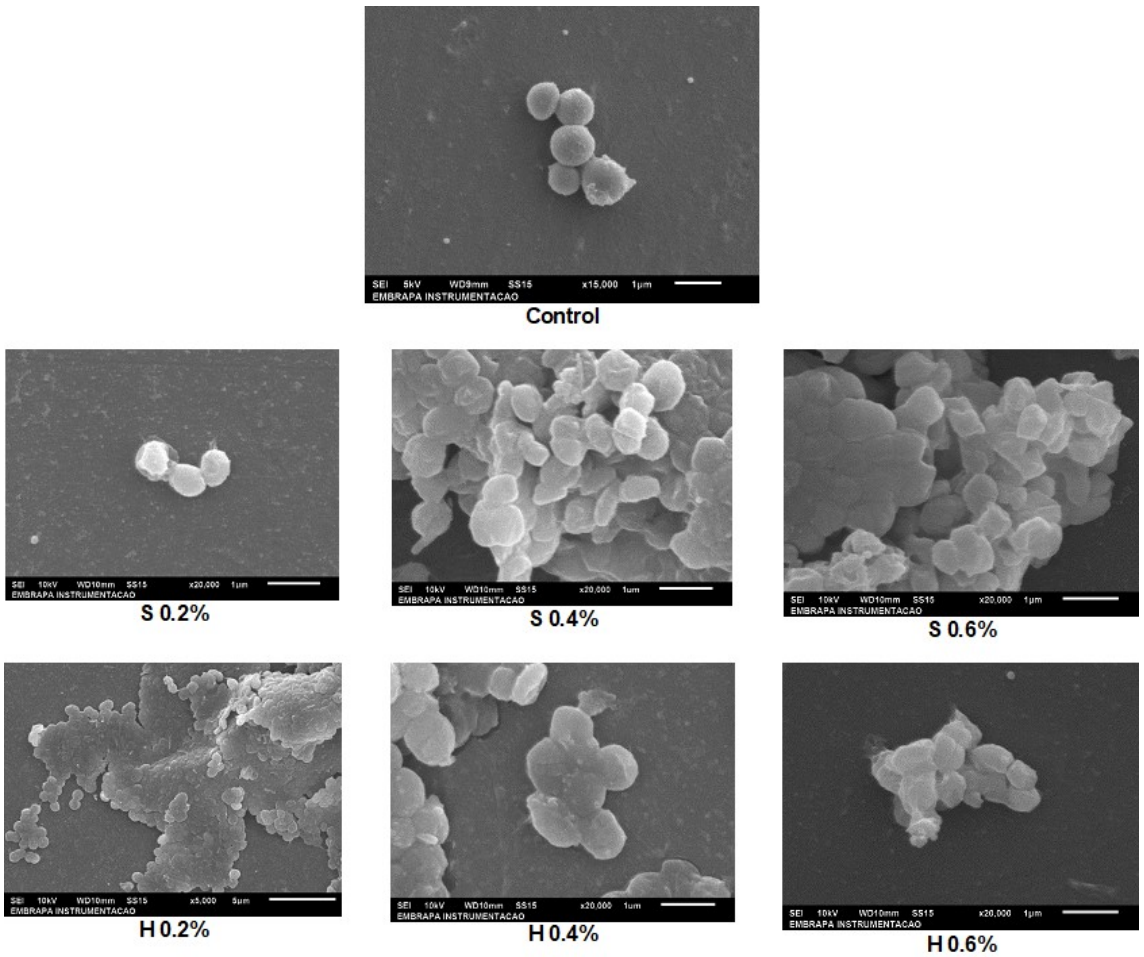

Fig. 16. *S. aureus* after 24h of contact with control LLDPE film and with LLDPE film with AgNPs + SiO_2 and AgNPs + HAP.

.

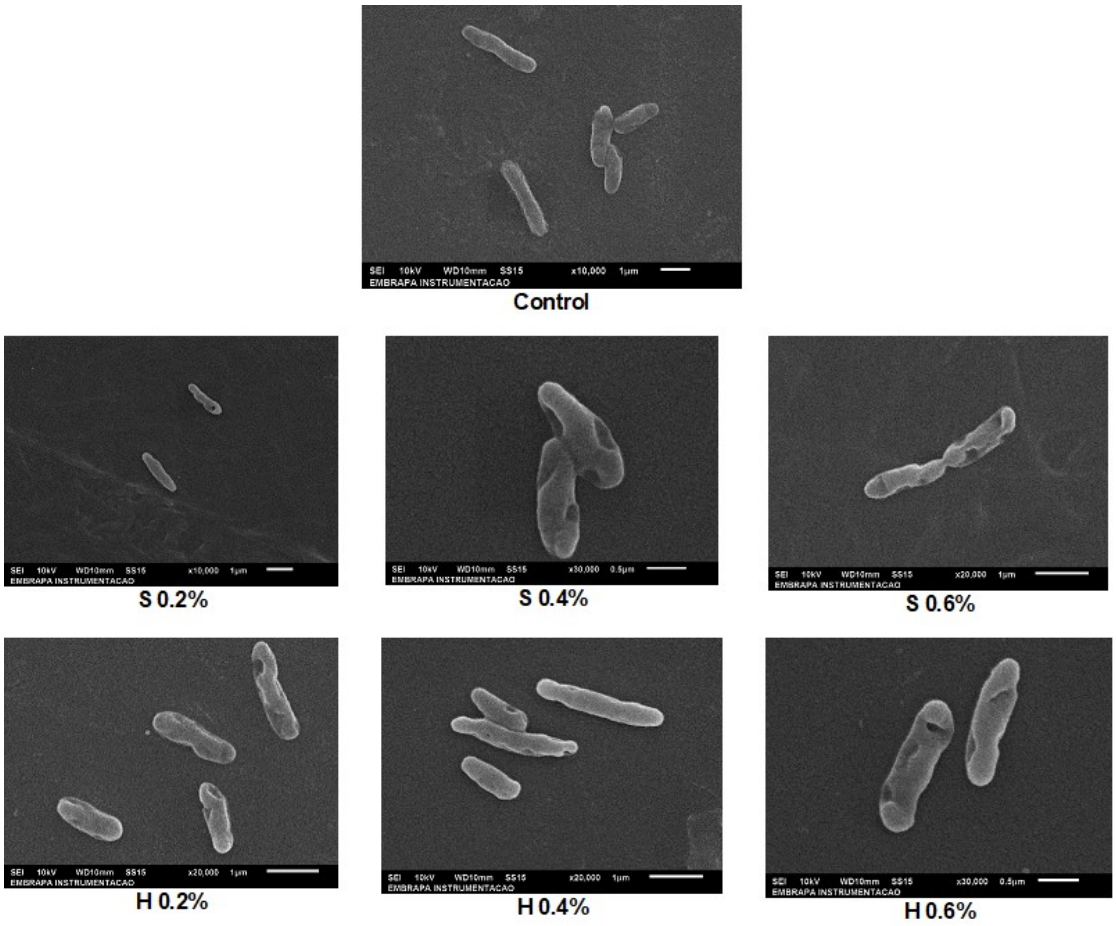

Fig. 17. *E. coli* after 24h of contact with control LLDPE film and with LLDPE film with AgNPs + SiO_2 and AgNPs + HAP.

This fact corroborates the mechanisms of action of AgNPs detailed above, where both the interaction by electrostatic attraction and the oxidative stress promoted by ROS causes the formation of lesions in the wall, thus causing structural changes in the cell membrane, allowing the entry of silver ions that consequently promotes cell death (69,79,126–128).

3.3. Migration

By the migration analysis in non-acidic and acidic simulants, we observed that after 10 days at a temperature of 20 °C (Table 5), the values of AgNPs migrated were higher in the acid simulant than in non-acidic. Furthermore, the statistical difference in the silica and hydroxyapatite carriers

was in the highest concentration (0.6%). However, in both simulants, the average silver diffusion (µg/mL) is within limits established by Mercosul and the European Union, where the migration of silver nanoparticles into the food cannot exceed 0.05 mg/kg (130,131).

Table 5
Mean migration distribution data of LLDPE with AgNPs + SiO_2 and AgNPs + HAP (µg/L) in non-acidic medium (pH > 4.5) and in acidic medium (pH <4.5).

Concentrations (%)	**Base pH (mg/kg)**	**Acidic pH (mg/kg)**
S 0.2	0.000326 ± 0.12[a]	0.001410 ± 0.07[a]
S 0.4	0.000751 ± 0.13[b]	0.001506 ± 0.10[a]
S 0.6	0.000261 ± 0.09[a]	0.000958 ± 0.11[b]
H 0.2	0.000254 ± 0.01[a]	0.000869 ± 0.05[a]
H 0.4	0.000400 ± 0.02[b]	0.000856 ± 0.04[a]
H 0.6	0.000469 ± 0.04[b]	0.002659 ± 0.20[b]

*Mean values followed by the same letter (a, b, c or d) within the same column do not differ significantly, as indicated by Duncan tests (p>0.05).

The migration of nanoparticles, including metallic ones, is influenced by extrinsic variables that can help on enhancing diffusions, such as the decrease in the pH of the medium (acidic) and the increase in time/temperature of contact with the food product, which stimulates the release of silver ions (132,133). In this study, it was observed that the highest migration values of silver to the simulants were in the acidic medium compared to basic. Furthermore, this diffusion process into the medium may have aided the relatively high temperature and period (20 °C and 10 days). Nevertheless, the results are below the established migration of silver nanoparticles into the food.

Conclusion.

The films with the composite AgNPS + carrier (SiO_2 or HAP) presented a percentage of inhibition higher than 90% against all investigated microorganisms in most concentrations. The antimicrobial action was more

effective in Gram-positive bacteria (*S. aureus*) being HAP carrier also more efficient in antimicrobial action on Gram-negative (*E.* coli) bacteria and fungi (*P.expansum* and *F. solani*), possibly due to its smaller size than the silica carrier that also favorable particle dispersion. Additionally, it can be stated that AgNPs into LLDPE films did not change the chemical and thermal properties of the films and migration values for both carries are within the limits of Mercosul and European Union. Therefore, HAP can be considered as a potential substitute for silica as a carrier for silver nanoparticles, and a promising alternative in food packaging.

Funding sources

This work was supported by Fundação de Amparo à Pesquisa do Estado de São Paulo (FAPESP), Conselho Nacional de Desenvolvimento Científico e Tecnológico/MCTI-SisNano (CNPq/442575/2019-0) and Research Fellowship (CNPq/310728/2019-3), Coordenação de Aperfeiçoamento de Pessoal de Nível Superior – Brasil- CAPES (Finance Code 001), Empresa Brasileira de Pesquisa Agropecuária (EMBRAPA, Project 13.16.04.041.00.00) and Rede Agronano-EMBRAPA from Brazil.

Capítulo 2.

Microbiological and physical-chemical evaluation of the efficiency of silver nanoparticles on the shelf-life extension of coconut water

Sabrina da Costa Brito[ab]
Vinicius Alex Cano Pereira[cb]
Ítalo Calisto[db]
Saad Barbar Netto[e]
Carlos Eduardo Formigoni[e]
Murilo Daniel de Mello Innocentini[e]
Milene Corso Mitsuyuki[b]
Kátia Sivieri[a]
Marcos David Ferreira[ba]

[a]Postgraduate Program in Food Science and Engineering, São Paulo State University "Julio de Mesquita Filho", Rod. Araraquara Jaú, Km 01, zip code: 14800-903, Araraquara, SP, Brazil.
[b]Embrapa Instrumentação, Rua XV de Novembro, 1452, zip code: 13560-970, São Carlos - SP, Brazil.
[c]Biotechnology Graduate Program, Federal University of São Carlos, Rod. Washington Luís, Km 235 – C. P.676, zip code: 13.565-905, São Carlos - SP, Brazil.
[d]Chemistry Graduate Program, University of Sao Paulo, Av. Trabalhador São-carlense, 400, zip code: 13.560-970, São Carlos - SP, Brazil.
[e]Postgraduate Program in Environmental Technology, Ribeirão Preto University, Av. Costábile Romano, 2201, zip code: 14096-900, Ribeirão Preto, SP, Brazil.
[f]Postgraduate Program in Chemistry, Federal University of São Carlos, Rod. Washington Luís, Km 235 – C. P.676, zip code: 13.565-905, São Carlos - SP, Brazil.

Abstract

This study intended to verify potential of using silver nanoparticles (AgNPs) dispersed in different carriers, silica (SiO_2) and hydroxyapatite (HAP), in food packaging in order to maintain the physicochemical and microbiological properties of pasteurized coconut water, at temperatures above recommended and after opening the package for consumption. Coconut water was packaged in linear low-density polyethylene (LLDPE) packages without compositive and with silver nanoparticles (AgNPs) dispersed in SiO_2 and HAP carriers at different concentrations (0.4 and 0.6 %). After filling and sealing these packages, they were refrigerated at 7 °C and analyzed within a period of 35 days, the physical and chemical analyzes carried out were pH, titratable acidity, soluble solids content, color, turbidity, phenolic compounds, antioxidant activities, reducing and non-reducing sugars, minerals and migrated silver. Microbiological analyzes were performed for the presence of psychrotrophic, molds and yeasts, enterobacteria and *Salmonella* spp. The addition of silver nanoparticles in polymer packaging, regardless of the type of carrier, maintained the physical and chemical characteristics of coconut water over the 35 days of refrigerated storage, furthermore provided a reduction of the microbial load of the product and the packaging with nanoparticles did not provide migration of silver for food. Therefore, the packages were effective in maintaining the physical, chemical and microbiological quality of the coconut water, being able to and extended five more days its shelf life at refrigeration temperatures higher than recommended.

Keywords: nanotechnology; silver nanoparticles; antimicrobial; food packaging, coconut water.

1. Introduction

Coconut, scientifically known as *cocos nucifera* L., is a fruit classified as a single-seeded drupe, which varies in shape from spherical to oval, and contains a thick fibrous outer shell and a hard inner shell (6). Internally, this fruit has two edible parts, the white core (pulp) and the liquid endosperm (coconut water), being the latter valued in the global market in 2021 at US$ 5 billion and could be worth US$ 11.72 billion in 2027. The appreciation of this product in the market is due to the growing demand of consumers who are more aware of the benefits of its consumption for health, being its commercialization in the ready-to-eat version in tetra park packs and plastic bottles (1,6,13).

Coconut water, which represents approximately 25% of the fruit's weight, is a drink with a slightly sweet and acidic taste (pH 4.6 - 5.6) and it is colorless (6,17,20). It has sugars, minerals, vitamins, phytohormones and amino acids. In addition, its consumption can have antioxidant, cardioprotective, anticancer and hypoglycemic action, providing benefits to the consumer's health (17,19,20).

When the liquid is in the hermetic cavity of the fruit it is in its sterile form, though it deteriorates easily when extracted and exposed to the air. Its deterioration can be caused by the activities of microorganisms, physical contaminants and poor storage conditions, besides the enzymatic activities which are higher during the handling of this product (3–7).

The decrease in the quality of coconut water results in a short shelf life and loss of its sensory (rancidity, turbidity and brown pigments) and nutritional properties, as well as presenting a health risk to the consumer due to bacterial infections and mycotoxins from fungi (6,7,23).

Currently a method to control the quality of coconut water is by heat treatment, such as pasteurization, which performs a reduction of microorganisms in six decimal cycles and the inactivation of the enzymatic activities. Nevertheless, it is interesting to use a combination of pasteurization with another method in order to optimize the quality conservation of this product, resulting in the extension of its shelf life (7,28,134).

With High Temperature Short Time (HTST) pasteurization, the coconut water is submitted to heating that does not exceed 100 C° in a period of seconds, providing 30 days of storage of this product at a maximum refrigeration temperature of 5°C, without altering its sensorial and microbiological characteristics (28).

However, a deficiency in temperature control is observed in refrigerated displays in Brazilian supermarkets with displays with 6 to 10 °C can be found storing foods such as milk and meat, this lack of control over cold storage can causing the loss of sensory and microbiological qualities of coconut water. Therefore, a technology applied to the packaging of this product becomes appealing. (30,135–137).

New technologies have been presented in packaging, which help to maintain the physicochemical and microbiological quality, optimizing food safety in addition to increasing the shelf life of the product (8,10).

One of the technologies in packaging is the incorporation of antimicrobial agents in nanoscale in the polymer structure, prompting an excellent effectiveness in reducing food spoilage and optimizing food safety (9–12,138,139).

Silver stands out among the antimicrobials studied for polymeric packaging

in food, especially those in nanoscale (9,45,46,140). Silver has a broader spectrum of antimicrobial activity against Gram-positive and Gram-negative bacteria, as well as fungi, when compared to other metallic particles (9,46,50–53,139). Its performance can be optimized, when it is in nanoscale, due to the increased proportion of atoms on the surface, thus increasing its antimicrobial action (47–49,54,55,139).

However, the nanoscale of silver is no guarantee for efficient antimicrobial performance, as it also depends on the uniformity and dispersion of the nanoparticles (52,55). Silver nanoparticles have a high tendency to form agglomerates due to the instability resulting from the large surface area/volume. In order to avoid this, silver is synthesized with an inorganic carrier, such as silica or hydroxyapatite, both have the characteristic of not causing cytotoxicity in the human body (51–53,56,58,80,81,87,88).

The present work aimed perform the first research in the literature that investigated the potential of using nanotechnology in food packaging in order to maintain the physicochemical and microbiological properties after coconut water´s pasteurization, especially in environments where temperature control conditions are ineffective and after the product has been opened for consumption.

2. Materials and Methodology

2.1. Materials

Pasteurized coconut water was obtained refrigerated from a company based in the state of Espírito Santo, Brazil, the pasteurization parameters were heating at 85°C for 30 seconds and regeneration at 6°C; the original packaging

of this coconut water is made of Polyethylene terephthalate without nanoparticles or other antimicrobial compound, the shelf life of the product is estimated in 30 days and after opened for 2 days, considering being refrigerated at 5°C, in this research they were stored at temperatures above recommended. The LLDPE packages with AgNPs + SiO_2 and AgNPs + HAP as well as the control were produced in the laboratories of Embrapa Instrumentação, based in the state of São Paulo, Brazil.

2.2. Sample Preparation

Upon receipt of the refrigerated coconut water, they were taken to a cold chamber (4-5 °C), where they were filled (25 mL) in bags with dimensions of 10 x 8 cm. These packages are LLDPE, with silver nanoparticle (AgNPs) and different carriers, silica (SiO2) and hydroxyapatite (HAP), which were prepared in different concentrations of AgNPs + SiO2 (S 0.4 and 0.6%) and AgNPs + HAP (H 0.4 and 0.6%) and compared to control package (films without nanoparticles). After filling and sealing these packages, they were refrigerated at 7 °C.

2.3. Physicochemical analysis

The refrigerated samples were analyzed in triplicate ever 7 days at 0, 7, 14, 21, 28 and 35 days.

The pH values were obtained using a Quimis Q400A bench pH meter. The titratable acidity it was determined from the titration under stirring of 5 mL of sample, along with 25 mL of distilled water and 0.3 mL of phenolphthalein solution. The results were expressed in grams of citric acid per 100 mL. The

soluble solids content it was quantified by an Atago RX-5000 cx bench refractometer. The results were expressed in °Brix.

Color determination was performed using a HunterLab MiniScan XE Plus colorimeter, with the samples evaluated in the L, a* and b* (color space) system proposed by the “Comission Internationale de l'Èclairage (CIE)”. The results were expressed in luminosity (L*).

To determine turbidity, first the absorbance at 610 nm was read by an Ultraviolet-Visible Spectrometer (UV-VIS) (Shimadzu UV 1650), and then the transmittance value (Tc) was obtained by calculating (141):

$$Tc = (10^{-A}) \times 100$$

A - Absorbance

The turbidity (T) (141):

$$T = 100 - Tc$$

The phenolic compounst, it was determined by the Folin-Ciocalteu spectrophotometric method, with absorbance reading at 725 nm by Ultraviolet-Visible Spectrometer (UV-VIS) (Shimadzu UV 1650). The results were expressed in mg gallic acid/100 mL. Antioxidant activities, was determined by the 2,2-diphenyl-1-picrylhydrazyl radical (DPPH) capture method by antioxidants, with absorbance reading at 515 nm by the Ultraviolet–Visible Spectrometer (UV-VIS) (Shimadzu UV 1650). Results were expressed as % inhibition of the DPPH radical (142):

$$\% \text{ of DPPH radical inhibition} = [(A_{control} - A_{sample}) / A_{control} \times 100]$$

The reducing and non-reducing sugars, it has been quantified by reverse phase HPLC-PDA (ACQ Arc Sys Core 1, Waters) on a Carbohydrate

- WAT084038 10 µm column (300 mm x 3.9 mm i.d., Waters, Milford, MA), with the mobile phase consisting of acetonitrile/ ultrapure water 80:20 (v/v), at a flow rate of 1.0 mL min-1. The determination was performed according to retention time and similarity of absorption spectrum with glucose, fructose and sucrose standards. The results were expressed in g 100 g-1 of sugars (143).

The quantification of minerals (calcium, magnesium, phosphorus, potassium, sodium, selenium, copper, iron, manganese and zinc) and silver in coconut water was performed using ICP OES (Thermo iCAP 6000 series – Dual view), in λ from 181.972 to 766.491nm.

The quantification of oxygen transmission rate (OTR [cm^3/m^2.d.bar]) was performed with a pressure-decay method based on Darcy's law derived from the manometric method of pressure accumulation in a closed volume proposed by the standards ASTM D 1434, ISO 2556 and ISO 15105-1, to analyze plastic films. The main difference is that here the data recorded refer to the pressure decay in a pressurized chamber as the gas permeates through the membrane to an atmospheric chamber. According to this testing procedure, a flat membrane is fixed between two chambers. The upstream chamber is pressurized with a fixed amount of pure gas, while the downstream chamber is kept at atmospheric pressure, even though with same gas composition of the pressurized chamber to avoid counter-diffusion of contaminants. Thus, both concentration and pressure gradients are created between the two chambers, inducing the flow of the component through the membrane. Pressure in the upstream chamber decays continuously with time. The gas sed for the experiments was oxygen (O2, 99.9% purity, White Martins, Brazil). The

complete procedure and mathematical analysis of the collected data are described elsewhere (144).

2.3. Microbiological Analysis

The refrigerated samples were analyzed in triplicate, at 0, 7, 14, 21, 28 and 35 days. The analyses were on psychrotrophic microorganisms, molds and yeasts, enterobacteria and *Salmonella* spp, where the results were expressed in Log $_{10}$ CFU/ mL. The procedures that were used for the analysis are:

- Psychrotrophic : inoculation of 0.1 mL of sample on Trypticase Soy Agar (spread plate method), and incubated at 7 °C/10 days (145,146).
- Molds and yeasts: inoculation of 0.1 mL of sample on Dichloran Rose Bengal Chloramphenicol agar (spread plate method), and incubated at 25°C /5 days (146,147).
- Enterobacteria: inoculation of 1 mL of sample on Violet Red Bile Glucose Agar (pour plate method), and incubated at 36 °C/24 hours (148)
- *Salmonella* spp : inoculation of 0.1 and 1 ml of sample in Rappaport-Vassilidis Soya Broth and Muller-Kauffmann Tetrathionate-Novobiocin Broth respectively, for follow-up of the microorganism´s biochemical and serological confirmation stages (149).

Statistical analysis

The analyses were performed by calculating the relative difference between the last and first assessments (physical and chemical from day zero to 35th and microbiological from day 7 to 35th). The values obtained were submitted to Bartlett's test to verify the condition of homogeneity of variance

between treatments. In cases of homogeneity, parametric ANOVA and Duncan's multiple range test comparisons were applied and for cases of heterogeneity, nonparametric ANOVA and test of Kruskal - Wallis multiple comparisons were used. The significance level adopted was 5%. The software used in the analysis was R version 4.1.0.

3. Results and Discussion

3.1. Physical and Chemical Analysis

In the physical and chemical analysis performed in this work, we could observe that with regard to pH (Table 1), there was no significant difference in any of the variables throughout the days of storage. The same could be verified in other studies regarding coconut water´s shelf life, and this stability may be due to protein´s denaturation during pasteurization (150–153).

Table 1
Distribution of pH mean data on days 0, 7, 14, 21, 28 - 35, and relative difference percentage (35 to 0 days) of LLDPE control, AgNPs + SiO_2 and AgNPs + HAP.

	Days						
Concentrations (%)	**0**	**7**	**14**	**21**	**28**	**35**	**Dif. % (std)**
Control	4.78	4.68	4.85	4.85	4.70	4.87	1.99 (0.79)[a]
S 0.4	4.76	4.81	4.89	4.89	4.84	4.91	3.08 (1.09)[a]
S 0.6	4.74	4.77	4.91	4.91	4.77	4.92	3.63 (0.14)[a]
H 0.4	4.79	4.82	4.92	4.92	4.96	4.93	2.78 (0.18)[a]
H 0.6	4.77	4.81	4.88	4.88	4.81	4.93	3.37 (0.21)[a]

*Mean values followed by the same letter (a) within the same column do not differ significantly, as indicated by Kruskal – Wallis tests (p≥0.05).
*Relative difference percentage calculation formula: (value on the 35th day - value on day 7)/ (value on day 7)*100.

Regarding the titratable acidity, a slight increase during storage was observed in all samples, however, no statistical difference was observed between samples, as shown in Table 2. Increase in acidity in the samples can be attributed to the production of free acids (151–153).

Table 2
Distribution of titratable acidity mean data (g/100mL) on days 0, 7, 14, 21, 28 –35, and relative difference percentage (35 to 0 days) of LLDPE control, AgNPs + SiO_2 and AgNPs + HAP.

	Days						
Concentrations (%)	**0**	**7**	**14**	**21**	**28**	**35**	**Dif. %**
Control	0.58	0.58	0.54	0.54	0.55	0.59	1.72 (4.75)[a]
S 0.4	0.55	0.56	0.56	0.56	0.56	0.59	4.21 (5.46)[a]
S 0.6	0.56	0.55	0.55	0.55	0.57	0.60	4.93 (6.32)[a]
H 0.4	0.55	0.55	0.57	0.57	0.56	0.57	2.83 (1.87)[a]
H 0.6	0.54	0.55	0.57	0.57	0.54	0.59	7.28 (2.22)[a]

*Mean values followed by the same letter (a or b) within the same column do not differ significantly, as indicated by Duncan tests (p≥0.05).
*Relative difference percentage calculation formula: (value on the 35th day - value on day 7)/ (value on day 7)*100.

Soluble solids showed small changes over the 35-day period. However, a slight decrease in °Brix can be observed in all samples when compared to day zero (Table 3), and the control one had a significant difference with the other samples. This result may be related to the consumption of sugars by microorganisms during the storage period, reflecting this higher decrease in the control film, which was not noticed antimicrobial additive, as we can verify in the microbiological results of this research (table 10-12) (44,152).

Table 3
Distribution of soluble solids mean data (°Brix) on days 0, 7, 14, 21, 28 - 35, and relative difference percentage (35 to 0 days) of LLDPE control, AgNPs + SiO_2 and AgNPs + HAP.

	Days						
Concentrations (%)	**0**	**7**	**14**	**21**	**28**	**35**	**Dif. % (std)**
Control	6.86	5.26	5.15	5.15	5.30	5.27	2.00 (0.54)[a]
S 0.4	6.74	5.30	5.26	5.26	5.27	5.32	5.66 (1.28)[b]
S 0.6	6.54	5.26	5.26	5.26	5.36	5.40	7.33 (5.01)[b]
H 0.4	5.70	5.25	5.25	5.25	5.27	5.33	11.00 (0.55)[c]
H 0.6	5.63	5.27	5.26	5.26	5.14	5.31	14.00 (0.12)[d]

*Mean values followed by the same letter (a, b, c or d) within the same column do not differ significantly, as indicated by Kruskal –Wallis tests (p≥0.05).
*Relative difference percentage calculation formula: (value on the 35th day - value on day 7)/ (value on day 7)*100.

Regarding the color (luminosity - L*), a slight decrease in luminosity could be verified in all samples during storage, with the coconut water packed in the control package showing a greater decrease in this parameter when compared to the other variables (Table 4).

Table 4
Distribution of color mean data (Luminosity -L*) on days 0, 7, 14, 21, 28 - 35, and relative difference percentage (35 to 0 days) of LLDPE control, AgNPs + SiO_2 and AgNPs + HAP.

	Days						
Concentrations (%)	**0**	**7**	**14**	**21**	**28**	**35**	**Dif. % (std)**
Control	96.40	95.07	95.12	92.94	92.99	90.24	-20.68 (5.62)[a]
S 0.4	95.40	94.73	95.12	94.59	93.98	93.48	-12.49 (2.15)[b]
S 0.6	95.06	93.00	96.13	96.13	95.19	94.68	-10.90 (1.23)[b]
H 0.4	93.78	93.96	94.15	96.90	95.91	94.28	-10.12 (1.83)[b]
H 0.6	93.26	92.81	96.08	95.98	96.16	95.62	-11.23 (4.31)[b]

*Mean values followed by the same letter (a or b) within the same column do not differ significantly, as indicated by Duncan tests (p≥0.05).
*Relative difference percentage calculation formula: (value on the 35th day - value on day 7)/ (value on day 7)*100.

The slight decrease in luminosity may be correlated with the increase in the turbidity of the samples, as we can be observed in Table 5, where the control sample had a greater increase in this parameter when compared to the other variables. The decrease in luminosity and increase in turbidity are related to the increase in microbial load and other cellular debris, as well as the gradual formation of insoluble complexes (150,152,153).

Table 5
Distribution of turbidity mean data on days 0, 7,14, 21, 28 - 35, and relative difference percentage (35 to 0 days) of LLDPE control, AgNPs + SiO_2 and AgNPs + HAP.

	Days						
Concentrations (%)	**0**	**7**	**14**	**21**	**28**	**35**	**Dif. % (std)**
Control	4.45	7.41	9.84	12.23	13.37	14.86	14.00 (17.05)[a]
S 0.4	5.79	7.67	7.95	7.55	8.96	9.98	3.00 (21.22)[b]
S 0.6	4.69	6.79	7.13	7.50	8.96	10.39	7.50 (40.86)[bc]
H 0.4	3.89	7.84	7.55	7.36	8.45	10.33	10.50 (18.79)[c]
H 0.6	5.35	7.97	7.32	7.98	8.52	10.37	5.00 (22.49)[c]

*Mean values followed by the same letter (a, b or c) within the same column do not differ significantly, as indicated by Duncan tests (p≥0.05).
*Relative difference percentage calculation formula: (value on the 35th day - value on day 7)/ (value on day 7)*100.

Regarding the phenolic compounds, it was verified that they showed a slight decrease throughout the storage period (Table 6), nonetheless not showing a significant difference between variables, but it was found that most samples potted in packages with nanoparticles did not show phenolic compound losses, unlike the control sample. The same could be observed in

others studies of coconut water´s shelf-life, that associate this reduction with an increase in microbial activity (150–152).

Table 6
Distribution of phenolic compounds mean data (mg gallium acid/100mL) of DPPH capture in percentage (%) on days 0, 7, 14, 21, 28 - 35, and relative difference percentage (35 to 0 days) of LLDPE control, AgNPs + SiO_2 and AgNPs + HAP.

	Days						
Concentrations (%)	**0**	**7**	**14**	**21**	**28**	**35**	**Dif. % (std)**
Control	0.0972	0.0920	0.0940	0.0905	0.0905	0.0887	-5.58 (3.21)[a]
S 0.4	0.0932	0.0913	0.0995	0.0989	0.0949	0.0869	1.89 (1.93)[a]
S 0.6	0.0980	0.0904	0.0900	0.0923	0.0871	0.0876	7.44 (13.78)[a]
H 0.4	0.0936	0.0927	0.0938	0.0910	0.0920	0.0886	-0.97 (5.47)[a]
H 0.6	0.0945	0.0963	0.0951	0.0902	0.0855	0.0807	1.99 (4.28)[a]

*Mean values followed by the same letter (a, b or c) within the same column do not differ significantly, as indicated by Duncan tests (p≥0.05).
*Relative difference percentage calculation formula: (value on the 35th day - value on day 7)/ (value on day 7)*100.

The reduction of phenolic compounds by microbial growth has coincided with the decrease in antioxidant capacity, mainly in the control sample, as it can be seen in Table 7 of DPPH radical capture by antioxidants, as the antioxidant activity depends on the composition and amount of bioactive compounds. (150). Decrease in these two variables during refrigerated storage of coconut water is in line with other studies (150–152).

Table 7
Distribution of DPPH radical inhibition mean data in percentage (%) on days 0, 7, 14, 21, 28 – 35, and relative difference percentage (35 to 0 days) of LLDPE control, AgNPs + SiO_2 and AgNPs + HAP.

	Days						
Concentrations (%)	**0**	**7**	**4**	**21**	**28**	**35**	**Dif. % (std)**
Control	83.50	62.24	54.98	58.10	53.66	54.70	-0.08 (0.012)[a]
S 0.4	82.28	63.30	59.50	50.48	53.61	60.86	-0.07 (0.010)[a]
S 0.6	82.55	63.60	58.10	60.93	60.80	57.68	-0.06 (0.006)[a]
H 0.4	82.53	63.67	56.11	61.64	58.55	58.34	-0.06 (0.010)[a]
H 0.6	83.67	64.31	56.62	62.13	55.37	55.99	-0.07 (0.003)[a]

*Mean values followed by the same letter (a, b or c) within the same column do not differ significantly, as indicated by Duncan tests (p≥0.05).
*Relative difference percentage calculation formula: (value on the 35th day - value on day 7)/ (value on day 7)*100.

Regarding reducing and non-reducing sugars, it can be verified that there was no significant difference between the samples (control and with

nanoparticles). Though, it can be observed that for glucose and sucrose, there was a reduction in their concentrations throughout the storage period, corroborating the results in coconut water in the research carried out by Chutia & Mahanta (2021) , Ma et al. (2019) and Mahnot et al. (2019) .

Table 8
Distribution of reducing and non-reducing sugars mean data (mg/ mL) on days 0, 7, 14, 21, 28 - 35, and relative difference percentage (35 to 0 days) of LLDPE control, AgNPs + SiO_2 and AgNPs + HAP.

	Days						
Concentrations (%)	**0**	**7**	**14**	**21**	**28**	**35**	**Dif % (std)**
	Fructose						
Control	73.30	79.18	72.23	74.67	77.21	71.24	-2.79 (3.74)[a]
S 0.4	67.89	72.23	76.35	65.70	77.07	75.01	10.75 (5.88)[a]
S 0.6	71.17	71.42	67.41	71.15	75.27	78.38	10.23 (12.29)[a]
H 0.4	71.34	72.51	65.13	72.29	69.22	75.54	5.90 (3.02)[a]
H 0.6	81.82	78.77	74.26	74.12	71.29	73.57	2.54 (11.04)[a]
	Glucose						
Control	65.24	60.22	61.00	61.98	57.88	57.19	-4.90 (5.87)[a]
S 0.4	62.90	61.79	60.02	59.18	56.61	53.46	6.27 (5.32)[a]
S 0.6	60.31	62.58	58.98	58.24	55.09	57.71	6.22 (11.86)[a]
H 0.4	60.63	59.00	59.11	57.99	53.12	55.30	2.77 (2.96)[a]
H 0.6	67.93	63.87	60.17	59.24	57.35	58.37	-1.05 (11.35)[a]
	Sucrose						
Control	3.56	3.16	3.98	-	-	-	5.50 (0.51)[a]
S 0.4	5.74	2.80	-	-	-	-	2.67 (5.91)[ab]
S 0.6	3.80	2.59	-	-	-	-	7.00 (23.58)[ab]
H 0.4	2.92	2.52	2.12	-	-	-	9.67 (7.82)[ab]
H 0.6	3.20	3.33	-	-	-	-	12.00 (12.00)[a]

*Mean values followed by the same letter (a or b) within the same column do not differ significantly, as indicated by Duncan and Kruskal –Wallis (sucrose) tests (p≥0.05).
*Relative difference percentage calculation formula: (value on the 35th day - value on day 7)/ (value on day 7)*100.

Regarding the concentration of minerals analyzed in this research, it was verified that there was no statistical difference between coconut water packed in control and those packed in packages with nanoparticles. In addition, there was no significant increase or decrease in micronutrient concentrations throughout the storage period (Table 9). With respect to silver, no migration of the composite to food was detected by the analysis.

Table 9
Distribution of mineral mean data (Ca, Mg, P, K, Na and Se) in mg/L on days 0, 7, 14, 21, 28 - 35, and relative difference percentage (35 to 0 days) of LLDPE control, AgNPs + SiO_2 and AgNPs + HAP.

Concentrations (%)	Days						
	0	7	14	21	28	35	Dif % (std)
	Calcium (Ca)						
Control	450.48	695.51	822.97	876.67	899.61	711.53	65.30 (54.81)[a]
S 0.4	621.38	748.88	894.96	824.53	676.79	768.91	24.84 (29.02)[a]
S 0.6	573.58	729.36	829.95	734.39	856.39	710.80	29.10 (36.19)[a]
H 0.4	713.70	773.83	877.92	783.06	847.41	772.73	8.38 (2.66)[a]
H 0.6	787.96	709.95	851.49	671.80	876.90	724.89	-7.89 (4.40)[a]
	Magnesium (Mg)						
Control	44.47	54.31	49.67	51.99	49.45	49.39	- 13.88 (26.59)[a]
S 0.4	53.77	57.52	54.05	46.72	39.37	47.81	-10.91 (7.85)[a]
S 0.6	49.96	57.64	49.76	45.61	49.64	42.38	-15.15 (1.15)[a]
H 0.4	53.36	55.95	48.81	51.74	56.51	43.86	-17.75 (1.35)[a]
H 0.6	60.10	52.51	51.11	43.50	50.71	52.50	-12.46 (2.62)[a]
	Phosphorus (P)						
Control	62.09	91.56	106.09	115.93	116.02	92.18	52.80 (40.26)[a]
S 0.4	80.70	99.48	116.04	110.61	88.03	96.79	21.11 (27.71)[a]
S 0.6	77.04	96.37	108.45	98.33	110.25	85.39	14.05 (2.34)[a]
H 0.4	93.53	102.98	113.93	102.34	109.63	97.83	4.69 (1.79)[a]
H 0.6	103.10	92.28	111.65	87.00	115.42	89.96	-12.67 (3.56)[a]
	Potassium (K)						
Control	6732.61	9253.98	10221.27	10761.04	10816.09	9555.78	62.40 (54.90)[a]
S 0.4	8715.11	9747.93	10839.34	10287.51	9232.16	9825.60	21.56 (26.05)[a]
S 0.6	8062.23	9648.43	10254.67	9653.06	10580.02	9190.76	27.84 (30.50)[a]
H 0.4	9371.25	10000.85	10574.69	10023.43	10658.10	9833.52	4.05 (4.15)[a]
H 0.6	10039.29	9397.07	10562.52	9141.44	10879.59	9548.16	1.50 (4.70)[a]
	Sodium (Na)						
Control	191.46	293.54	343.48	367.75	372.52	306.46	66.54 (51.92)[a]
S 0.4	259.88	313.45	374.36	348.59	291.10	320.51	24.36 (27.63)[a]
S 0.6	241.20	307.46	353.44	313.19	355.86	296.02	26.01 (28.09)[a]
H 0.4	293.58	328.02	368.93	327.51	359.31	323.58	10.43 (4.07)[a]
H 0.6	327.61	301.70	360.09	341.06	370.22	309.56	-5.39 (4.53)[a]
	Selenium (Se)						
Control	44.43	58.33	69.26	74.47	78.05	65.88	50.09 (27.32)[a]
S 0.4	55.33	64.26	74.99	74.28	67.88	70.37	27.65 (18.17)[a]
S 0.6	53.86	61.48	71.88	69.92	75.06	66.57	26.41 (26.38)[a]
H 0.4	63.46	64.42	73.99	69.67	74.38	70.93	11.91 (3.87)[a]
H 0.6	67.40	63.48	73.74	63.62	77.76	65.76	-2.40 (2.37)[a]

*Mean values followed by the same letter (a or b) within the same column do not differ significantly, as indicated by Duncan tests ($p \geq 0.05$).
*Relative difference percentage calculation formula: (value on the 35th day - value on day 7)/ (value on day 7)*100.

Regarding the OTR it was observed in Figs. 1 and 2 that there was no statistical difference between the LLDPE and LLDPE with nanoparticles, ranging in average from 4345 to 4380 cm^3/m^2.d.bar, which is much lower than

the range reported by Ahmed et al. for LLDPE reinforced with ZnO nanoparticles (154). This behavior is favorable, since this polymer type has high-barrier properties for packaging applications (155). Nevertheless, it was verified that the samples 0.6% AgNPs + SiO_2 (4380 cm^3/m^2.d.bar) and 0.4% AgNPs + HAP (4652 cm^3/m^2.d.bar) showed slightly lower values of OTR. According to Ahmed et al., it is commonly believed that a longer path caused by addition of nanoparticles through a section of film results in a decrease in gas transmission. In addition, the interface and the free volume of the region surrounding the particles also contribute to the decreased OTR of nanocomposite films. The slightly higher values of OTR for the other samples could be due to the complex natures of the nanoparticles and its effect on decreasing the cohesion forces with the polymer matrix (43,154,156).

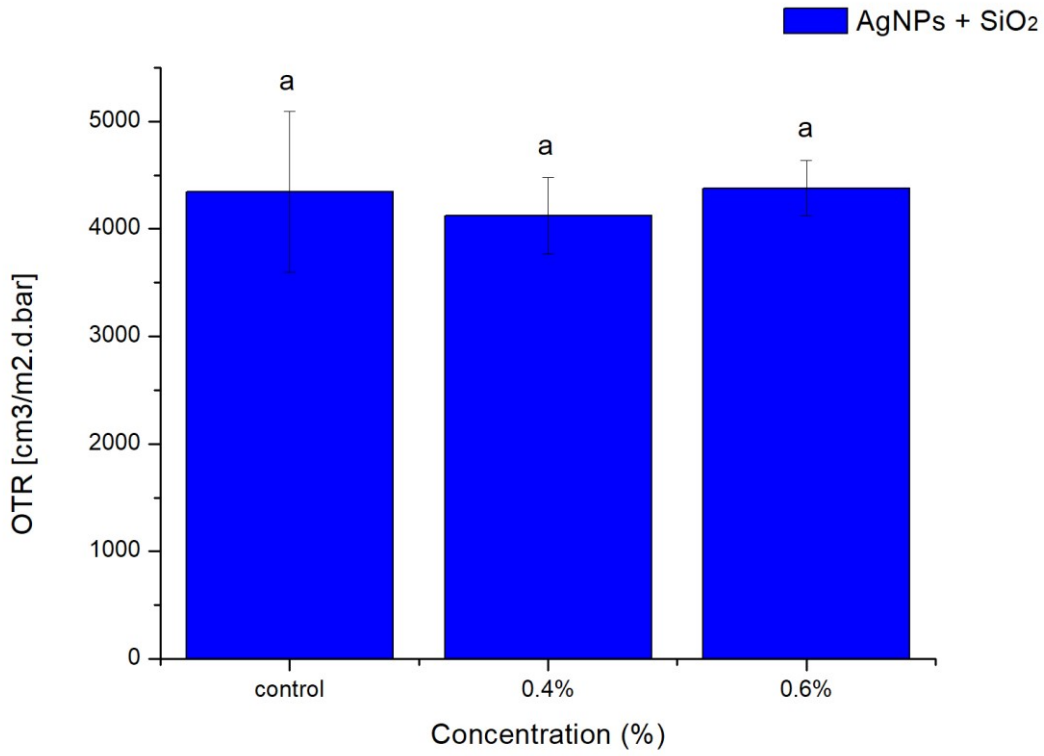

Fig. 1. Oxygen transmission rate (OTR [cm3/m2.d.bar]) of control and nanostructured (SiO_2) samples: control, 0.4% and 0.6%.

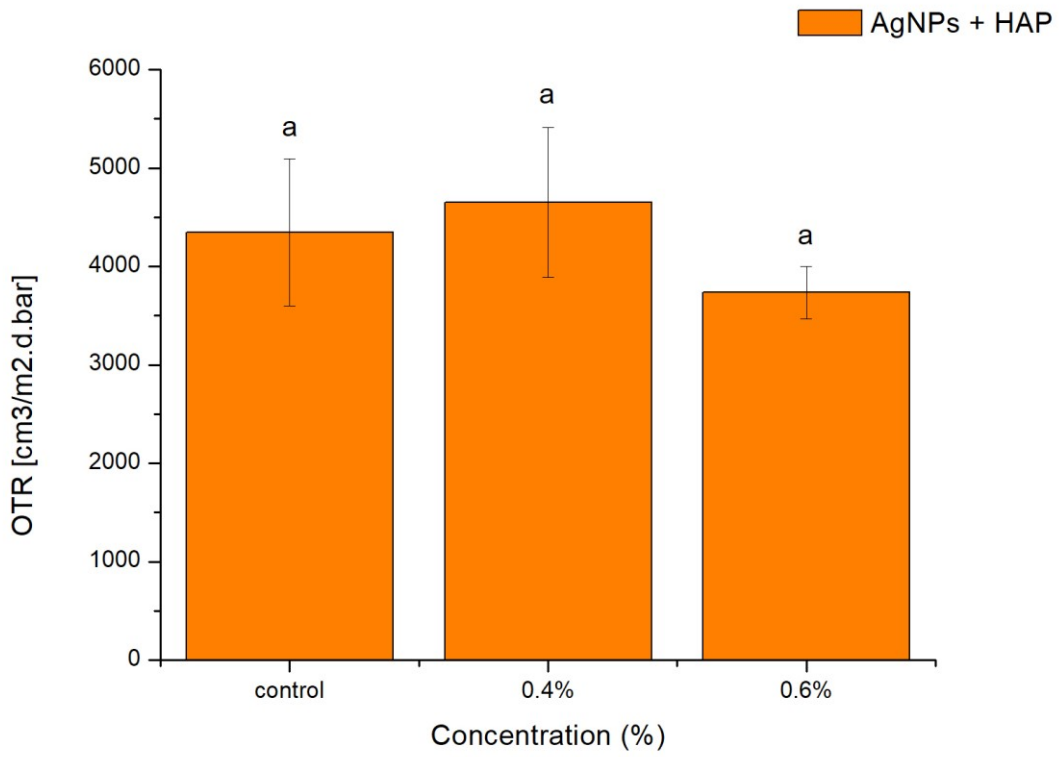

Fig. 2. Oxygen transmission rate (OTR [cm3/m2.d.bar]) of control and nanostructured (HAP) samples: control, 0.4% and 0.6%.

3.1. Microbiological Analysis

Among the microorganisms analyzed, psychrotrophs are characterized as cold-tolerant bacteria that grow in foods under refrigeration, and are able to produce visible growth at 7 °C from seven to ten days (145).

In the present research, it was observed (Table 10) that there was no growth in the period of seven days, corroborating the aforementioned period. However, after 14 days of storage the growth of psychrotrophs was verified only in the coconut water conditioned in the control package, thus being able to determine that the packages with AgNPs + SiO_2 and AgNPs + HAP were efficient in containing the growth of this bacterium over 21 days. Nevertheless, from 28 days onwards the psychrotrophs began to appear in the samples with

nanoparticles, but always with a lower growth rate than the control sample. Among the films with nanoparticles, it was observed that that the samples of AgNPs + HAP did not present a significant difference compared to the control sample, however, they present a lower microbial growth than the control sample, showing that all samples with nanoparticles have an effective microbiological reduction.

Table 10
Distribution of logarithmic growth mean data (CFU/ mL) of Psychrotrophs on days 7, 14, 21, 28 - 35, and relative difference percentage (35 to 7 days) of LLDPE control, AgNPs + SiO_2 and AgNPs + HAP.

	Days					
Concentrations (%)	**7**	**14**	**21**	**28**	**35**	**Dif. % (std)**
Control	-	4.222	4.523	4.921	5.602	5.58 (0.13)[a]
S 0.4	-	-	-	4.824	4.921	4.69 (1.40)[b]
S 0.6	-	-	-	4.222	4.824	3.23 (1.40)[b]
H 0.4	-	-	-	4.523	4.699	4.89 (0.17)[ab]
H 0.6	-	-	-	4.222	4.523	4.89 (0.17)[ab]

*Mean values followed by the same letter (a or b) within the same column do not differ significantly, as indicated by Duncan tests (p≥0.05).
*Relative difference percentage calculation formula: (value on the 35th day - value on day 7)/ (value on day 7)*100.

Regarding molds and yeasts, in the present research the growth of molds was observed, but not of yeasts. In the case of this microorganism, its presence was confirmed from the period of seven days (Table 11). Indeed, there was a more significant growth in the coconut water packed in the control film during all storage period than in the films with nanoparticles, showing the efficiency of the antimicrobial action of the compound in the packaging under coconut water.

Table 11
Distribution of log growth mean data (CFU/ mL) of molds on days 7, 14, 21, 28 - 35, and relative difference percentage (35 to 7 days) of LLDPE control, AgNPs + SiO_2 and AgNPs + HAP.

	Days					
Concentrations (%)	**7**	**14**	**21**	**28**	**35**	**Dif. % (std)**
Control	5.000	5.067	5.398	5.426	5.426	5.67 (0.11)[a]
S 0.4	4.523	4.523	5.067	4.921	4.523	4.95 (0.24)[b]
S 0.6	4.222	4.523	4.523	4.523	4.523	4.89 (0.17)[b]
H 0.4	4.222	4.699	4.699	4.523	4.523	4.79 (0.17)[b]
H 0.6	4.699	4.523	4.523	4.824	4.222	5.05 (0.10)[b]

*Mean values followed by the same letter (a or b) within the same column do not differ significantly, as indicated by Duncan tests (p≥0.05).
*Relative difference percentage calculation formula: (value on the 35th day - value on day 7)/ (value on day 7)*100.

In relation to enterobacteria, their presence was determined in most of the samples during the seven-day period and their growth was continuous throughout the 35 days of storage (Table 12). The coconut water bottled in the control packaging showed a greater microbial growth but did not present significant difference with the samples packed in films with nanoparticles of higher concentration, with AgNPs + SiO_2 and AgNPs + HAP at a concentration of 0.4 % being the most effective in containing microbial growth, this result may be related to the agglomeration of nanoparticles observed by FEG-SEM in samples with higher concentration.

Table 12
Distribution of logarithmic growth mean data (CFU/ mL) of enterobacteria on days 7, 14, 21, 28 - 35, and relative difference percentage (35 to 7 days) of LLDPE control, AgNPs + SiO_2 and AgNPs + HAP.

	Days					
Concentrations (%)	**7**	**14**	**21**	**28**	**35**	**Dif. % (std)**
Control	5.602	6.151	6.151	6.190	6.595	6.59 (0.07)^{a}
S 0.4	5.501	5.584	6.108	6.041	6.472	6.34 (0.08)^{bc}
S 0.6	5.336	5.544	5.855	5.875	6.267	6.44 (0.03)^{ab}
H 0.4	5.398	5.713	6.035	6.007	6.450	6.25 (0.11)^{c}
H 0.6	5.000	5.740	5.740	5.885	6.346	6.46 (0.06)^{ab}

*Mean values followed by the same letter (a, b or c) within the same column do not differ significantly, as indicated by Duncan tests (p≥0.05).
*Relative difference percentage calculation formula: (value on the 35th day - value on day 7)/ (value on day 7)*100.

During the 35-day storage period of the coconut water under refrigeration, *Salmonella* spp was absent in all samples, LLDPE control, AgNPs + SiO_2 and AgNPs + HAP.

Even though most of the microorganisms analyzed were detected in the research, they are within the acceptable microbiological standards of Brazilian legislation for the commercialization of juices and other beverages submitted to technological processes for microbial reduction, as well as by Food and Drug

Administration (FDA) for the pasteurization of fresh juices that must achieve a 5 log reduction on the population of relevant pathogenic microorganisms. Therefore, in this study the microbial growth values were lower than the values established in the legislation (32,157).

In this research, it was observed a reduction in microbial growth and an optimization of the physical and chemical qualities of coconut water bottled in packages that contain polymer with silver nanoparticles, refrigerated at a temperature above that recommended for this type of product. These results corroborate with other studies which have also used polymer packaging with AgNPs in chicken meat (46), banana (158), papaya (159) and carrot (140).

The mechanisms of microbiological inhibition of AgNPs, although not well elucidated, may be associated with damage to the microbial cell wall and membrane, increase in reactive oxygen species (ROS), penetration and consequent intracellular damage (9,126,139).

The interaction between silver ions and microorganisms begins with their adhesion to the cell wall and cell membrane, promoting morphological changes leading to a disorder of permeability and respiratory functions due to a depolarization of the membrane. All this action can lead to cell death (9,127,128,139). This disorder in the microbiological wall and membrane enables the entry of silver ions into the cell, interacting with DNA and proteins. In relation to DNA, nanoparticles change their shape from relaxed to condensed, disabling the DNA to replicate whereas with proteins, ions interact with thiol groups of enzymes, especially of the respiratory chains (9,52,129,139).

With regard to ROS, are oxygen with a strong redox potential. Which under normal conditions, ROS production and antioxidant capacity in the cell are balance. However, when the ROS molecules get in contact with the silver ions an imbalance is formed in their antioxidant capacity and promotes an increase in ROS production. All this causes redox to favor oxidation, leading to oxidative stress, in order to overcome this stress cells exhibit protective responses of defense mechanisms, promoting damage to the cell wall and biomolecules such as proteins, lipids and DNA, leading to cell death (9,69,79,126,128,139)

Conclusion

From this study, it was possible to observe that the main quality features of coconut water were maintained with the addition of AgNPs in LLDPE films, regardless of the type of the carrier (silica or hydroxyapatite), during refrigerated storage, extending shelf life from 30 to 35 days, even after opening the original packaging and at temperatures above 5 °C, what is the recommended temperature for refrigeration of this food product. It also can ben stated that this is related to the reduction of microbial load corroborating the microbiological results.

The films with AgNPs + SiO_2 and AgNPs + HAP also did not show significant differences between carriers in microbial inhibition; however we can conclude that even the film with low concentration is effective to inhibit microbial growth at rates below that considered permitted in this type of food by Brazilian and international legislation, and with that keep the physical and chemical quality of coconut water.

In addition, the packaging did not provide detectable amounts of silver migration into the food product. As the first work on polymer packaging with silver nanoparticles for coconut water, we can conclude in this first results that polymeric packaging with low concentrations of silver nanoparticles, regardless of the carrier, can be effective in provide maintenance of quality in coconut water, in all variables, even after opening for consumption and at temperatures above 5 °C.

Acknowledgments

The authors would like to thank the financial support provided by Fundação de Amparo à Pesquisa do Estado de São Paulo (FAPESP), Conselho Nacional de Desenvolvimento Científico e Tecnológico/MCTI-SisNano (CNPq/442575/2019-0) and Research Fellowship (CNPq/310728/2019-3, 382640/2022-5), Coordenação de Aperfeiçoamento de Pessoal de Nível Superior – Brasil- CAPES (Finance Code 001), Empresa Brasileira de Pesquisa Agropecuária (EMBRAPA, Project 13.16.04.041.00.00) and Rede Agronano-EMBRAPA from Brazil. The authors also thank Green Coco Ltda, in name of Mr. Gamaliel Pires de Moura for supplying the water coconut samples for this research, Embrapa Pecuária and Unaerp for collaborating in the analyzes carried out in this research, and Nanox for supplying the pellets AgNPs + SiO_2.

Considerações Finais

As embalagens poliméricas contendo AgNPs + SiO_2 e AgNPs, + HAP foram eficazes na contenção do crescimento microbiano como mostrado

nas análises *in vitro* como na água de coco. No caso do produto alimentício, esta ação antimicrobiana refletiu em melhores resultados físico-química ao longo de 35 dias, portanto estas embalagens com nanopartículas, independente do carregador, possibilitou que a água de coco ter uma vida de prateleira com qualidade além dos 30 dias estipulados para o produto e em refrigeração acima da recomendada ideal pela legislação, além disso estas embalagens não promoveram migração de seus aditivos para o alimento, portanto demostrando que as nanopartículas de prata pode ter um grande potencial de uso em garrafas para água de coco como também para outras bebidas pasteurizadas.

Referências

1. Research D. Global Coconut Water Market: Analysis By Type, By Form, By Packaging, By Distribution Channel, By Region, Size and Trends with Impact of COVID-19 and Forecast up to 2027 [Internet]. September. 2022 [cited 2022 Jan 2]. p. 139. Available from: https://www.reportlinker.com/p06325451/Global-Coconut-Water-Market-Analysis-By-Type-By-Form-By-Packaging-By-Distribution-Channel-By-Region-Size-and-Trends-with-Impact-of-COVID-19-and-Forecast-up-to.html?utm_source=GNW
2. Maria Simone de Castro Pereira Brainer. Coco: produção e mercado. Cad Setorial ETENE. 2021;(206):1–13.
3. Bhullar MS, Patras A, Kilanzo-Nthenge A, Pokharel B, Yannam SK, Rakariyatham K, et al. Microbial inactivation and cytotoxicity evaluation of UV irradiated coconut water in a novel continuous flow spiral reactor.

Food Res Int [Internet]. 2018;103:59–67. Available from: http://dx.doi.org/10.1016/j.foodres.2017.10.004

4. Ochoa-Velasco CE, Díaz-Lima MC, Ávila-Sosa R, Ruiz-López II, Corona-Jiménez E, Hernández-Carranza P, et al. Effect of UV-C light on Lactobacillus rhamnosus, Salmonella Typhimurium, and Saccharomyces cerevisiae kinetics in inoculated coconut water: Survival and residual effect. J Food Eng. 2018;223:255–61.
5. Segura-Badilla O, Lazcano-Hernández M, Kammar-García A, Vera-López O, Aguilar-Alonso P, Ramírez-Calixto J, et al. Use of coconut water (Cocus nucifera L) for the development of a symbiotic functional drink. Heliyon. 2020;6(3).
6. Naik M, Sunil CK, Rawson A, Venkatachalapathy N. Tender Coconut Water : A Review on Recent Advances in Processing and Preservation Tender Coconut Water : A Review on Recent Advances in Processing and Preservation. Food Rev Int [Internet]. 2020;00(00):1–22. Available from: https://doi.org/10.1080/87559129.2020.1785489
7. Donsingha S, Assatarakul K. Kinetics model of microbial degradation by UV radiation and shelf life of coconut water. Food Control. 2018;92:162–8.
8. Bahrami A, Delshadi R, Assadpour E, Jafari SM, Williams L. Antimicrobial-loaded nanocarriers for food packaging applications. Adv Colloid Interface Sci. 2020;278.
9. Brito S da C, Bresolin JD, Sivieri K, Ferreira MD. Low-density polyethylene films incorporated with silver nanoparticles to promote antimicrobial efficiency in food packaging. Food Sci Technol Int. 2020;1–

14.

10. Mousavi Khaneghah A, Hashemi SMB, Limbo S. Antimicrobial agents and packaging systems in antimicrobial active food packaging: An overview of approaches and interactions. Food Bioprod Process. 2018;111:1–19.
11. Han JW, Ruiz-Garcia L, Qian JP, Yang XT. Food Packaging: A Comprehensive Review and Future Trends. Compr Rev Food Sci Food Saf. 2018;17(4):860–77.
12. Galli R, Hall MC, Breitenbach ER, Colpani GL, Zanetti M, de Mello JMM, et al. Antibacterial polyethylene - Ethylene vinyl acetate polymeric blend by incorporation of zinc oxide nanoparticles. Polym Test. 2020;89(April).
13. Prades A, Dornier M, Diop N, Pain JP. Coconut water preservation and processing: A review. Fruits. 2012;67(3):157–71.
14. Yin CS. Coconut Handbook. Liu S, editor. Singapore: Tetra Pak South East Asia Pte Ltd; 2016. 186 p.
15. Penha E das M, Cabral LMC, Matta VM da. Água de coco. In: Venturini WG, editor. Bebidas não alcoólicas: Ciência e tecnologia. 1st ed. São Paulo: Blucher; 2010. p. 1–12.
16. Naik M, Sunil CK, Rawson A, Venkatachalapathy N. Tender Coconut Water: A Review on Recent Advances in Processing and Preservation. Food Rev Int [Internet]. 2022;38(6):1215–36. Available from: https://doi.org/10.1080/87559129.2020.1785489
17. Biswas K, Mohanta YK, Kumar VB, Hashem A, Fathi Abd_Allah E, Mohanta D, et al. Nutritional assessment study and role of green silver nanoparticles in shelf-life of coconut endosperm to develop as functional food. Saudi J Biol Sci [Internet]. 2020;27(5):1280–8. Available from:

https://doi.org/10.1016/j.sjbs.2020.01.011

18. Rajashri K, Rastogi NK, Negi PS. Non- thermal Processing of Tender Coconut Water - A Review. Food Rev Int [Internet]. 2020; Available from: https://doi.org/10.1080/87559129.2020.1847142

19. Beristaín-Bauza S, Martínez-Niño A, Ramírez-González AP, Ávila-Sosa R, Ruíz-Espinosa H, Ruiz-López II, et al. Inhibition of Salmonella Typhimurium growth in coconut (Cocos nucifera L.) water by hurdle technology. Food Control. 2018;92:312–8.

20. Rajashri K, Roopa BS, Negi PS, Rastogi NK. Effect of ozone and ultrasound treatments on polyphenol content, browning enzyme activities, and shelf life of tender coconut water. J Food Process Preserv. 2020;44(3):1–11.

21. Camargo Prado F, De Dea Lindner J, Inaba J, Thomaz-Soccol V, Kaur Brar S, Soccol CR. Development and evaluation of a fermented coconut water beverage with potential health benefits. J Funct Foods [Internet]. 2015;12:489–97. Available from: http://dx.doi.org/10.1016/j.jff.2014.12.020

22. Kwiatkowski A, Oliveira DM, Clemente E. Atividade Enzimática e Paramêtros Fisico-Químicos de Água de Cocos Colhidos em Diferentes Estádios de Desenvolvimento e Estação Climática. Rev Bras Frutic. 2012;34(2):551–9.

23. Birkelund T, Johansen RF, Illum DG, Dyrskog SE, Østergaard JA, Falconer TM, et al. Fatal 3-nitropropionic acid poisoning after consuming coconut water. Emerg Infect Dis. 2021;27(1):278–80.

24. Cappelletti M, Ferrentino G, Endrizzi I, Aprea E, Betta E, Corollaro ML, et

al. High Pressure Carbon Dioxide pasteurization of coconut water: A sport drink with high nutritional and sensory quality. J Food Eng [Internet]. 2015;145:73–81. Available from: http://dx.doi.org/10.1016/j.jfoodeng.2014.08.012

25. Reddy KV, Das M, Das SK. NONTHERMAL STERILIZATION OF GREEN COCONUTWATER FOR PACKAGING. J Food Qual. 2007;30(2007):466–80.

26. Santos T. Pasteurização x Esterilização de alimentos: quais as diferenças? [Internet]. https://foodsafetybrazil.org/pasteurizacao-x-esterilizacao-quais-as-diferencas/. 2022. p. 1. Available from: https://foodsafetybrazil.org/pasteurizacao-x-esterilizacao-quais-as-diferencas/

27. Brasil. Instrução normativa n°9: Estabelece os padrões de identidade e qualidade para a água de coco, bem como os respectivos parâmetros analíticos. MAPA. 2020;22(1):38.

28. Abreu FAP de, Souza ACR de. Água de Coco Pasteurizada em Sistemas HTST: Fabricação em Pequenas e Médias Escalas de Processamento. Embrapa Agroindústria Trop. 2017;1:1–7.

29. Schmidt FL, Castro MFPMG, Ferracini H, Leitão MFF. Practices of making and application from the analysis of dangers and control critics points in the coconut water processing. Hig Aliment. 2004;18(121):65–76.

30. Montanhini MTM, Parades F. Storage temperature of pasteurized milk traded by supermarkets in Curitiba, Paraná. Vigilância Sanitária em Debate. 2015;3(5):94–8.

31. Silva SEL da, Paz DS, Bratifich KSB, Sebastião C, Silva L das G,

Rodrigues RA. Thermal storage of chilled broilers in supermarkets and the risk of transmission of Salmonella spp. Brazilian J Dev. 2020;6(11):87679–87.

32. Brasil. Resolução da diretoria colegiada- RDC Nº 331. Padrões microbiológicos de alimentos e sua aplicação. ANVISA. 2019;249:1–6.
33. Brody AL, Bugusu B, Han JH, Sand CK, McHugh TH. Innovative food packaging solutions. J Food Sci. 2008;73(8):107–16.
34. Gava AJ, Silva CAB, Frias JRG. Embalagem de Alimentos. In: Gava AJ, editor. Tecnologia de alimentos: princípios e aplicações. 2nd ed. São Paulo: Nobel; 2008. p. 105–27.
35. Manrich S. Processamento de termoplásticos. In: S M, editor. Processamento de termoplásticos. São Paulo: Artliber; 2005.
36. Piringer OG, Baner AL. Preservation of quality through packaging. In: Piringer OG, Baner AL, editors. Plastic Packaging Materials for Food: Barrier Function, Mass Transport, Quality Assurance, and Legislation. 1st ed. Weinheim: Wiley-VCH; 2000. p. 4–8.
37. Geueke B, Groh K, Muncke J. Food packaging in the circular economy: Overview of chemical safety aspects for commonly used materials. J Clean Prod. 2018;193:491–505.
38. Du W, Ren Y, Tang Y, Shi Y, Yao X, Zheng C, et al. Different structure transitions and tensile property of LLDPE film deformed at slow and very fast speeds. Eur Polym J [Internet]. 2018;103(April):170–8. Available from: https://doi.org/10.1016/j.eurpolymj.2018.04.003
39. Yaqub N, Farooq WA, AlSalhi MS. Nonlinear optical properties of LLDPE composites with titanium dioxide anatase phase. J King Saud Univ - Sci

[Internet]. 2022;34(1):101723. Available from: https://doi.org/10.1016/j.jksus.2021.101723

40. Chaudhari BC, Khanderay J, Patil C, Patil AM, Joshi SA, Singh V, et al. Waste Eggshells for the Decoration of Carbon Nanotubes and Graphene Nanosheets with Hydroxyapatite for Preparation of LLDPE Nanocomposites. J Polym Environ [Internet]. 2019;27(11):2352–9. Available from: https://doi.org/10.1007/s10924-019-01501-3

41. Panrong T, Karbowiak T, Harnkarnsujarit N. Effects of acetylated and octenyl-succinated starch on properties and release of green tea compounded starch/LLDPE blend films. J Food Eng [Internet]. 2020;284(February):110057. Available from: https://doi.org/10.1016/j.jfoodeng.2020.110057

42. Medeiros GR, Ferreira SRS, Carciofi BAM. High pressure carbon dioxide for impregnation of clove essential oil in LLDPE films. Innov Food Sci Emerg Technol. 2017;41:206–15.

43. Ahmed J, Mulla M, Arfat YA, Bher A, Jacob H, Auras R. Compression molded LLDPE films loaded with bimetallic (Ag-Cu) nanoparticles and cinnamon essential oil for chicken meat packaging applications. Lwt [Internet]. 2018;93(March):329–38. Available from: https://doi.org/10.1016/j.lwt.2018.03.051

44. Becaro AA, Puti FC, Panosso AR, Gern JC, Brandão HM, Correa DS, et al. Postharvest Quality of Fresh-Cut Carrots Packaged in Plastic Films Containing Silver Nanoparticles. Food Bioprocess Technol. 2016;9(4):637–49.

45. Abutalib MM, Rajeh A. Enhanced structural, electrical, mechanical

properties and antibacterial activity of Cs/PEO doped mixed nanoparticles (Ag/TiO2) for food packaging applications. Polym Test [Internet]. 2021;93:107013. Available from: https://doi.org/10.1016/j.polymertesting.2020.107013

46. Ahmed J, Mulla M, Arfat YA, Bher A, Jacob H, Auras R. Compression molded LLDPE films loaded with bimetallic (Ag-Cu) nanoparticles and cinnamon essential oil for chicken meat packaging applications. Lwt [Internet]. 2018;93(October 2017):329–38. Available from: https://doi.org/10.1016/j.lwt.2018.03.051
47. Roduner E. Size matters: Why nanomaterials are different. Chem Soc Rev. 2006;35(7):583–92.
48. Hochella MF. Nanoscience and technology: The next revolution in the Earth sciences. Earth Planet Sci Lett. 2002;203(2):593–605.
49. Waychunas GA. Structure, aggregation and characterization of nanoparticles. Rev Mineral Geochemistry. 2001;44(1):105–66.
50. Becaro AA, Puti FC, Correa DS, Paris EC, Marconcini JM, Ferreira MD. Polyethylene Films Containing Silver Nanoparticles for Applications in Food Packaging: Characterization of Physico-Chemical and Anti-Microbial Properties. J Nanosci Nanotechnol [Internet]. 2015;15(3):2148–56. Available from: http://openurl.ingenta.com/content/xref?genre=article&issn=1533-4880&volume=15&issue=3&spage=2148
51. Lazić V, Smičiklas I, Marković J, Lončarević D, Dostanić J, Ahrenkiel SP, et al. Antibacterial ability of supported silver nanoparticles by functionalized hydroxyapatite with 5-aminosalicylic acid. Vacuum.

2018;148:62–8.

52. Roy A, Butola BS, Joshi M. Synthesis, characterization and antibacterial properties of novel nano-silver loaded acid activated montmorillonite. Appl Clay Sci. 2017;146(February):278–85.

53. Zhou Q, Wang T, Wang C, Wang Z, Yang Y, Li P, et al. Synthesis and characterization of silver nanoparticles-doped hydroxyapatite/alginate microparticles with promising cytocompatibility and antibacterial properties. Colloids Surfaces A Physicochem Eng Asp. 2020;585(March 2019).

54. Damm C, Neumann M, Münstedt H. Properties of nanosilver coatings on polymethyl methacrylate. Soft Mater. 2005;3(2–3):71–88.

55. Olmos D, Pontes-Quero G, Corral A, González-Gaitano G, González-Benito J. Preparation and Characterization of Antimicrobial Films Based on LDPE/Ag Nanoparticles with Potential Uses in Food and Health Industries. Nanomaterials [Internet]. 2018;8(2):60. Available from: http://www.mdpi.com/2079-4991/8/2/60

56. Pawliszak P, Malina D, Sobczak-Kupiec A. Rhodiola rosea extract mediated green synthesis of silver nanoparticles supported by nanosilica carrier. Mater Chem Phys [Internet]. 2019;234(May):390–402. Available from: https://doi.org/10.1016/j.matchemphys.2019.05.027

57. Zhang X, Chaimayo W, Yang C, Yao J, Miller BL, Yates MZ. Silver-hydroxyapatite composite coatings with enhanced antimicrobial activities through heat treatment. Surf Coatings Technol. 2017;325:39–45.

58. Fereidoon A, Memarian S, Albooyeh A, Tarahomi S. Influence of mesoporous silica and hydroxyapatite nanoparticles on the mechanical

and morphological properties of polypropylene. Mater Des [Internet]. 2014;57:201–10. Available from: http://dx.doi.org/10.1016/j.matdes.2013.12.046

59. Coutinho FMB, Mello IL, Santa Maria LC de. Polietileno: principais tipos, propriedades e aplicações. Polímeros [Internet]. 2003;13(1):01–13. Available from: http://www.scielo.br/scielo.php?script=sci_arttext&pid=S0104-14282003000100005&lng=pt&tlng=pt

60. Galli R, Hall MC, Breitenbach ER, Colpani GL, Zanetti M, de Mello JMM, et al. Antibacterial polyethylene - Ethylene vinyl acetate polymeric blend by incorporation of zinc oxide nanoparticles. Polym Test. 2020;89(February).

61. Silva C, Bobillier F, Canales D, Sepúlveda FA, Cament A, Amigo N, et al. Mechanical and antimicrobial polyethylene composites with CaO nanoparticles. Polymers (Basel). 2020;12(9).

62. Muangprakaew P, Luangsa-Ard N, Komasatitaya J. Study of Physical, Mechanical, and Barrier Properties in Linear Low-Density Polyethylene Mixed with Silver Zeolite Nanoparticles (Ag-zeolite) Film. Indian J Sci Technol. 2021;14(31):2526–34.

63. Moniri Javadhesari S, Alipour S, Mohammadnejad S, Akbarpour MR. Antibacterial activity of ultra-small copper oxide (II) nanoparticles synthesized by mechanochemical processing against S. aureus and E. coli. Mater Sci Eng C [Internet]. 2019;105(110011):1–10. Available from: https://doi.org/10.1016/j.msec.2019.110011

64. Król A, Pomastowski P, Rafińska K, Railean-Plugaru V, Buszewski B.

Zinc oxide nanoparticles: Synthesis, antiseptic activity and toxicity mechanism. Adv Colloid Interface Sci. 2017;249:37–52.

65. Hoseinnejad M, Jafari SM, Katouzian I. Inorganic and metal nanoparticles and their antimicrobial activity in food packaging applications. Crit Rev Microbiol [Internet]. 2018;44(2):161–81. Available from: https://doi.org/10.1080/1040841X.2017.1332001

66. Duffy LL, Osmond-McLeod MJ, Judy J, King T. Investigation into the antibacterial activity of silver, zinc oxide and copper oxide nanoparticles against poultry-relevant isolates of Salmonella and Campylobacter. Food Control. 2018;92:293–300.

67. Siddiqi KS, Husen A, Rao RAK. A review on biosynthesis of silver nanoparticles and their biocidal properties. J Nanobiotechnology [Internet]. 2018;16(14):1–28. Available from: https://doi.org/10.1186/s12951-018-0334-5

68. Chougule SS, Gurme ST, Jadhav JP, Dongale TD, Tiwari AP. Low density polyethylene films incorporated with Biosynthesised silver nanoparticles using Moringa oleifera plant extract for antimicrobial, food packaging, and photocatalytic degradation applications. J Plant Biochem Biotechnol [Internet]. 2021;30(1):208–14. Available from: https://doi.org/10.1007/s13562-020-00584-7

69. Shen T, Wang Q, Li C, Zhou B, Li Y, Liu Y. Transcriptome sequencing analysis reveals silver nanoparticles antifungal molecular mechanism of the soil fungi Fusarium solani species complex. J Hazard Mater [Internet]. 2020;388(January):122063. Available from: https://doi.org/10.1016/j.jhazmat.2020.122063

70. Peighambardoust SJ, Zahed-Karkaj S, Peighambardoust SH, Ebrahimi Y, Peressini D. Characterization of carboxymethyl cellulose-based active films incorporating non-modified and Ag or Cu-modified Cloisite 30B and montmorillonite nanoclays. Iran Polym J (English Ed. 2020;29(12):1087–97.

71. Dehghani S, Peighambardoust SH, Peighambardoust SJ, Fasihnia SH, Khosrowshahi NK, Gullón B, et al. Optimization of the Amount of ZnO, CuO, and Ag Nanoparticles on Antibacterial Properties of Low-Density Polyethylene (LDPE) Films Using the Response Surface Method. Food Anal Methods. 2021;14(1):98–107.

72. Hajizadeh H, Peighambardoust SJ, Peighambardoust SH, Peressini D. Physical, mechanical, and antibacterial characteristics of bio-nanocomposite films loaded with Ag-modified SiO2 and TiO2 nanoparticles. J Food Sci. 2020;85(4):1193–202.

73. Mehr RK, Peighambardoust SJ, Peighambardoust SH. Preparation and Characterization of Corn Starch/Clay Nanocomposite Films: Effect of Clay Content and Surface Modific. Starch. 2018;70(3–4):1–41.

74. Castro-Mayorga JL, Fabra MJ, Pourrahimi AM, Olsson RT, Lagaron JM. The impact of zinc oxide particle morphology as an antimicrobial and when incorporated in poly(3-hydroxybutyrate-co-3-hydroxyvalerate) films for food packaging and food contact surfaces applications. Food Bioprod Process [Internet]. 2017;101:32–44. Available from: http://dx.doi.org/10.1016/j.fbp.2016.10.007

75. Malafatti JOD, Bernardo MP, Moreira FKV, Ciol H, Inada NM, Mattoso LHC, et al. Electrospun poly(lactic acid) nanofibers loaded with silver

sulfadiazine/[Mg–Al]-layered double hydroxide as an antimicrobial wound dressing. Polym Adv Technol. 2020;

76. Munhoz DR, Bernardo MP, Malafatti JOD, Moreira FKV, Mattoso LHC. Alginate films functionalized with silver sulfadiazine-loaded [Mg-Al] layered double hydroxide as antimicrobial wound dressing. Int J Biol Macromol. 2019;141.

77. Al-Shabib NA, Husain FM, Ahmad I, Khan MS, Khan RA, Khan JM. Rutin inhibits mono and multi-species biofilm formation by foodborne drug resistant Escherichia coli and Staphylococcus aureus. Food Control [Internet]. 2017;79:325–32. Available from: http://dx.doi.org/10.1016/j.foodcont.2017.03.004

78. Kim JH, Yoo JG, Ham JS, Oh MH. Direct detection of Escherichia coli, staphylococcus aureus, and Salmonella spp. in animal-derived foods using a magnetic bead-based immunoassay. Korean J Food Sci Anim Resour. 2018;38(4):727–36.

79. Alghuthaymi MA, Abd-Elsalam KA, Shami A, Said-Galive E, Shtykova E V., Naumkin A V. Silver/chitosan nanocomposites: Preparation and characterization and their fungicidal activity against dairy cattle toxicosis penicillium expansum. J Fungi. 2020;6(2).

80. Jeelani PG, Mulay P, Venkat R, Ramalingam C. Multifaceted Application of Silica Nanoparticles. A Review. Silicon. 2020;12(6):1337–54.

81. Mehmood A, Ghafar H, Yaqoob S, Gohar UF, Ahmad B. Mesoporous Silica Nanoparticles: A Review. J Dev Drugs. 2017;06(02).

82. Dong W, Su J, Chen Y, Xu D, Cheng L, Mao L, et al. Characterization and antioxidant properties of chitosan film incorporated with modified silica

nanoparticles as an active food packaging. Food Chem [Internet]. 2022;373(PA):131414. Available from: https://doi.org/10.1016/j.foodchem.2021.131414

83. Biswas MC, Tiimob BJ, Abdela W, Jeelani S, Rangari VK. Nano silica-carbon-silver ternary hybrid induced antimicrobial composite films for food packaging application. Food Packag Shelf Life [Internet]. 2019;19(March 2018):104–13. Available from: https://doi.org/10.1016/j.fpsl.2018.12.003

84. Wu C, Zhu Y, Wu T, Wang L, Yuan Y, Chen J, et al. Enhanced functional properties of biopolymer film incorporated with curcurmin-loaded mesoporous silica nanoparticles for food packaging. Food Chem [Internet]. 2019;288(January):139–45. Available from: https://doi.org/10.1016/j.foodchem.2019.03.010

85. Ciobanu CS, Iconaru SL, Le Coustumer P, Constantin LV, Predoi D. Antibacterial activity of silver-doped hydroxyapatite nanoparticles against gram-positive and gram-negative bacteria. Nanoscale Res Lett. 2012;7:1–9.

86. Loo SCJ, Moore T, Banik B, Alexis F. Biomedical Applications of Hydroxyapatite Nanocomposites. Curr Pharm Biotechnol. 2010;11(4):333–42.

87. Maghsoodi MR, Ghodszad L, Asgari Lajayer B. Dilemma of hydroxyapatite nanoparticles as phosphorus fertilizer: Potentials, challenges and effects on plants. Environ Technol Innov [Internet]. 2020;19:100869. Available from: https://doi.org/10.1016/j.eti.2020.100869

88. Nasrallah DA, Ibrahim MA. Enhancement of physico-chemical, optical, dielectric and antimicrobial properties of polyvinyl alcohol/carboxymethyl

cellulose blend films by addition of silver doped hydroxyapatite nanoparticles. J Polym Res [Internet]. 2022;29(3). Available from: https://doi.org/10.1007/s10965-022-02943-5

89. Sciena CR, dos Santos MF, Moreira FKV, Sena Neto AR, Marconcini JM, Correa DS, et al. Starch:Pectin Acidic Sachets Development for Hydroxyapatite Nanoparticles Storage to Improve Phosphorus Release. J Polym Environ [Internet]. 2019;27(4):794–802. Available from: http://dx.doi.org/10.1007/s10924-019-01391-5

90. Khalil MMH, Ismail EH, El-Baghdady KZ, Mohamed D. Green synthesis of silver nanoparticles using olive leaf extract and its antibacterial activity. Arab J Chem [Internet]. 2014;7(6):1131–9. Available from: http://dx.doi.org/10.1016/j.arabjc.2013.04.007

91. Pagno CH, Costa TMH, De Menezes EW, Benvenutti E V., Hertz PF, Matte CR, et al. Development of active biofilms of quinoa (Chenopodium quinoa W.) starch containing gold nanoparticles and evaluation of antimicrobial activity. Food Chem [Internet]. 2015;173:755–62. Available from: http://dx.doi.org/10.1016/j.foodchem.2014.10.068

92. Avila-Sosa R, Hernández-Zamoran E, López-Mendoza I, Palou E, Munguía MTJ, Nevárez-Moorillón GV, et al. Fungal inactivation by mexican oregano (lippia berlandieri schauer) essential oil added to amaranth, chitosan, or starch edible films. J Food Sci. 2010;75(3):127–33.

93. Spricigo PC, Trento JP, Bresolin JD. Methods of preparing flower stem samples for scanning electron microscopy. Adv Ornam Hortic an Landscaping. 2015;21(1):17–26.

94. Mendes L. D., Bresolin J.D., Assis O.B.G., Britto D. Avaliação in vitro da ação da quitosana e de seu derivado quaternizado na inibição do crescimento do fungo penicillium expansum. Brazilian J Biosyst Eng. 2016;10(1):116–28.

95. Raffi M, Mehrwan S. Investigations into the antibacterial behavior of copper nanoparticles against Escherichia coli. Ann Microbiol. 2010;60:75–80.

96. Labanni A, Zulhadjri, Handayani D, Ohya Y, Arief S. Size controlled synthesis of well-distributed nano-silver on hydroxyapatite using alkanolamine compounds. Ceram Int. 2020;46(5):5850–5.

97. Santos MAFE, Lôbo IP, Da Cruz RS. Synthesis and characterization of novel ZrO2-SiO2 mixed oxides. Mater Res. 2014;17(3):700–7.

98. Mendes AC, Maia LJQ, Paris EC, Siu Li M. Solvent effect on the optimization of 1.54 μm emission in Er-doped Y2O3-Al2O3-SiO2 powders synthesized by a modified Pechini method. Curr Appl Phys. 2013;13(8):1558–65.

99. Motaung T, Mochane M, Makhetha T, Motloung S, Mokhothu T, Mokhena T, et al. Effect of mechanical treatment on morphology and thermal and mechanical properties of sugar cane bagasse-low-density polyethylene composites. Polym Compos [Internet]. 2017;38(8):1497–503. Available from: http://doi.wiley.com/10.1002/pc.23717

100. Madani M. Structure, optical and thermal decomposition characters of LDPE graft copolymers synthesized by gamma irradiation. Curr Appl Phys [Internet]. 2011;11(1):70–6. Available from: http://dx.doi.org/10.1016/j.cap.2010.06.021

101. Wang YJ, Yan WD. Investigation on chain structure of LLDPE obtained by ethylene in-situ copolymerization with DSC and XRD. Chinese Sci Bull. 2007;52(6):736–42.

102. Lynch ME, Folz DC, Clark DE. Use of FTIR reflectance spectroscopy to monitor corrosion mechanisms on glass surfaces. J Non Cryst Solids. 2007;353(27):2667–74.

103. Gowri LAVS, Amorim T, Carneiro N, Souto AP, Esteves MF. Novel Copolymer for SiO2 Nanoparticles Dispersion. J Appl Polym Sci. 2011;124:1553–61.

104. Gieroba B, Przekora A, Kalisz G, Kazimierczak P, Song CL, Wojcik M, et al. Collagen maturity and mineralization in mesenchymal stem cells cultured on the hydroxyapatite-based bone scaffold analyzed by ATR-FTIR spectroscopic imaging. Mater Sci Eng C [Internet]. 2021;119(October 2020):111634. Available from: https://doi.org/10.1016/j.msec.2020.111634

105. Pereira FF, Paris EC, Bresolin JD, Foschini MM, Ferreira MD, Corrêa DS. Investigation of nanotoxicological effects of nanostructured hydroxyapatite to microalgae Pseudokirchneriella subcapitata. Ecotoxicol Environ Saf [Internet]. 2017;144(May):138–47. Available from: http://dx.doi.org/10.1016/j.ecoenv.2017.06.008

106. Mulla M, Ahmed J, Al-Attar H, Castro-Aguirre E, Arfat YA, Auras R. Antimicrobial efficacy of clove essential oil infused into chemically modified LLDPE film for chicken meat packaging. Food Control. 2017;73:663–71.

107. Canevarolo S V. Microscópia Eletrônica da Varredura. In: Canevarolo S

V, editor. Técnicas de Caracterização de Polímeros. 3rd ed. São Paulo: Artliber; 2017. p. 448.

108. Hemati F, Garmabi H. Compatibilised LDPE/LLDPE/nanoclay nanocomposites: I. Structural, mechanical, and thermal properties. Can J Chem Eng. 2011;89(1):187–96.

109. Al-Salem SM, Bumajdad A, Khan AR, Sharma BK, Chandrasekaran SR, Al-Turki FA, et al. Non-isothermal degradation kinetics of virgin linear low density polyethylene (LLDPE) and biodegradable polymer blends. J Polym Res. 2018;25(5).

110. Khonakdar HA. Dynamic mechanical analysis and thermal properties of LLDPE/EVA/modified silica nanocomposites. Compos Part B Eng [Internet]. 2015;76:343–53. Available from: http://dx.doi.org/10.1016/j.compositesb.2015.02.031

111. Boschetto DL, Lerin L, Cansian R, Pergher SBC, Di Luccio M. Preparation and antimicrobial activity of polyethylene composite films with silver exchanged zeolite-Y. Chem Eng J. 2012;204–205:210–6.

112. Pérez MA, Rivas BL, Garrido-Miranda KA, Campos-Requena VH, Martínez M, Castaño J, et al. Low Density Polyethylene (LDPE) nanocomposites with passive and active barrier properties. J Chil Chem Soc. 2014;59(2):2442–6.

113. Bumbudsanpharoke N, Lee W, Ko S. A Comprehensive Feasibility Study on the Properties of LDPE-Ag Nanocomposites for Food Packaging Applications. Polym Compos. 2018;39:3178–86.

114. Anh DH, Dumri K, Anh NT, Punyodom W, Rachtanapun P. Facile fabrication of polyethylene/silver nanoparticle nanocomposites with silver

nanoparticles traps and holds early antibacterial effect. J Appl Polym Sci. 2016;133(17):1–8.

115. Liang X, Sun M, Li L, Qiao R, Chen K, Xiao Q, et al. Preparation and antibacterial activities of polyaniline/Cu 0.05Zn 0.95O nanocomposites. Dalt Trans. 2012;41(9):2804–11.
116. Padmavathy N, Vijayaraghavan R. Enhanced bioactivity of ZnO nanoparticles - An antimicrobial study. Sci Technol Adv Mater. 2008;9(035004):1–7.
117. Russell AD. Similarities and differences in the responses of microorganisms to biocides. J Antimicrob Chemother. 2003;52(5):750–63.
118. Sondi I, Salopek-Sondi B. Silver nanoparticles as antimicrobial agent: A case study on E. coli as a model for Gram-negative bacteria. J Colloid Interface Sci. 2004;275(1):177–82.
119. Yamamoto O. Influence of particle size on the antibacterial activity of zinc oxide. Int J Inorg Mater. 2001;3(7):643–6.
120. Rahimi G, Alizadeh F, Khodavandi A. Mycosynthesis of silver nanoparticles from Candida albicans and its antibacterial activity against Escherichia coli and Staphylococcus aureus. Trop J Pharm Res. 2016;15(2):371–5.
121. Barzegar R, Safaei HR, Nemati Z, Ketabchi S, Talebi E. Green synthesis of silver nanoparticles using Zygophyllum qatarense Hadidi leaf extract and evaluation of their antifungal activities. J Appl Pharm Sci. 2018;8(3):168–71.
122. Matei A, Matei S, Matei G-M, Cogălniceanu G, Cornea CP. Biosynthesis of silver nanoparticles mediated by culture filtrate of lactic acid bacteria,

characterization and antifungal activity. EuroBiotech J. 2020;4(2):97–103.

123. Braga LR, Rangel ET, Suarez PAZ, Machado F. Simple synthesis of active films based on PVC incorporated with silver nanoparticles: Evaluation of the thermal, structural and antimicrobial properties. Food Packag Shelf Life. 2018;15(December):122–9.

124. Malandrakis AA, Kavroulakis N, Avramidou M, Papadopoulou KK, Tsaniklidis G, Chrysikopoulos C V. Metal nanoparticles: Phytotoxicity on tomato and effect on symbiosis with the Fusarium solani FsK strain. Sci Total Environ [Internet]. 2021;787:147606. Available from: https://doi.org/10.1016/j.scitotenv.2021.147606

125. Al-Otibi F, Perveen K, Al-Saif NA, Alharbi RI, Bokhari NA, Albasher G, et al. Biosynthesis of silver nanoparticles using Malva parviflora and their antifungal activity. Saudi J Biol Sci [Internet]. 2021;28(4):2229–35. Available from: https://doi.org/10.1016/j.sjbs.2021.01.012

126. Roy A, Bulut O, Some S, Mandal AK, Yilmaz MD. Green synthesis of silver nanoparticles: Biomolecule-nanoparticle organizations targeting antimicrobial activity. RSC Adv [Internet]. 2019;9(5):2673–702. Available from: http://dx.doi.org/10.1039/C8RA08982E

127. Din MI, Arshad F, Hussain Z, Mukhtar M. Green Adeptness in the Synthesis and Stabilization of Copper Nanoparticles: Catalytic, Antibacterial, Cytotoxicity, and Antioxidant Activities. Nanoscale Res Lett. 2017;12(638):1–15.

128. Happy Agarwal, Menon S, Venkat Kumar S, Rajeshkumar S. Mechanistic study on antibacterial action of zinc oxide nanoparticles synthesized using green route. Chem Biol Interact. 2018;286(November 2017):60–70.

129. Durán N, Durán M, de Jesus MB, Seabra AB, Fávaro WJ, Nakazato G. Silver nanoparticles: A new view on mechanistic aspects on antimicrobial activity. Nanomedicine Nanotechnology, Biol Med [Internet]. 2016;12(3):789–99. Available from: http://dx.doi.org/10.1016/j.nano.2015.11.016

130. Brasil - Ministério da Saúde. Resolução da Diretoria Colegiada- RDC Nº 326, de 3 de Dezembro de 2019-Estabelece a lista positiva de aditivos destinados à elaboração de materiais plásticos e revestimentos poliméricos em contato com alimentos e dá outras providências. DOU. 2019;1–163.

131. Carbone M, Donia DT, Sabbatella G, Antiochia R. Silver nanoparticles in polymeric matrices for fresh food packaging. J King Saud Univ - Sci [Internet]. 2016;28(4):273–9. Available from: http://dx.doi.org/10.1016/j.jksus.2016.05.004

132. Ahari H, Lahijani LK. Migration of silver and copper nanoparticles from food coating. Coatings. 2021;11(4).

133. Morais L de O, Macedo EV, Granjeiro JM, Delgado IF. Critical evaluation of migration studies of silver nanoparticles present in food packaging: a systematic review. Crit Rev Food Sci Nutr [Internet]. 2020;60(18):3083–102. Available from: https://doi.org/10.1080/10408398.2019.1676699

134. Adubofuor J, Amoah I, Osei-Bonsu I. Sensory and physicochemical properties of pasteurized coconut water from two varieties of coconut. Food Sci Qual Manag [Internet]. 2016;54(October):26–32. Available from: www.iiste.org

135. Silva SEL da, Paz DS, Bratifich KSB, Sebastião C, Silva L das G,

Rodrigues RA. Armazenamento Térmico De Frangos Resfriados Em Supermercados E O Risco De Transmissão De Salmonella Spp / Thermal Storage of Chilled Broilers in Supermarkets and the Risk of Transmission of Salmonella Spp. Brazilian J Dev. 2021;7(1):10503–12.

136. Silva-Júnior AC, Nascimento JF do, Tostes E do SL, Silva A do SS da. Análises microbiológicas de carne bovina moída comercializada em supermercados. Pubvet. 2018;12(10):1–7.
137. Bezerra Oliveira AM, Sobral DO, Beckmam KRL, Camargo LVE, Madalena NP, Zuniga ADG. Avaliacão Da Temperatura De Balcões Refrigerados De Supermercados De Palmas - To. DESAFIOS - Rev Interdiscip da Univ Fed do Tocantins. 2019;6(Especial):17–23.
138. Ebrahimi H, Abedi B, Bodaghi H, Davarynejad G, Haratizadeh H, Conte A. Investigation of developed clay-nanocomposite packaging film on quality of peach fruit (Prunus persica Cv. Alberta) during cold storage. J Food Process Preserv. 2018;42(2):1–9.
139. Brito S da C, Malafatti JOD, Arab FE, Bresolin JD, Paris EC, de Souza CWO, et al. One-pot synthesis of CuO, ZnO, and Ag nanoparticles: structural, morphological, and bactericidal evaluation. Inorg Nano-Metal Chem [Internet]. 2022;0(0):1–11. Available from: https://doi.org/10.1080/24701556.2022.2078358
140. Becaro AA, Puti FC, Panosso AR, Gern JC, Brandão HM, Correa DS, et al. Postharvest Quality of Fresh-Cut Carrots Packaged in Plastic Films Containing Silver Nanoparticles. Food Bioprocess Technol. 2016;9(4):637–49.
141. Horwitz W. Official Methods of Association of Official Analytical Chemists.

13th ed. Chemists A of OA, editor. Washington DC; 1980. 1044 p.

142. Cheng Z, Moore J, Yu L. High-throughput relative DPPH radical scavenging capacity assay. J Agric Food Chem. 2006;54(20):7429–36.

143. Chenlo F, Moreira R, Chaguri L, Torres MD. Effects of storage conditions on sugars and moisture content of whole chestnut fruits. J Food Process Preserv. 2010;34(4):609–20.

144. Innocentini MD de M, Formigoni CE. Rapid pressure-decay technique for determining the O2 and CO2 permeability coefficients of polymeric films considering the gas compressibility effect. Chem Eng Commun [Internet]. 2023 Mar 13;1–8. Available from: https://doi.org/10.1080/00986445.2023.2189108

145. Vasavada PC, F.J.Critzer. Psychrotrophic microrganisms. In: Salfinger Y, Tortorello ML, editors. Compendium of Methods for the Microbiological Examination of Foods. 5th ed. Washington: American Public Health Association; 2015. p. 175–89.

146. Frank JF, Yousef AE. Tests for groups of microrganisms. In: Frank JF, Wehr HM, editors. Standard Methods for the Examination of Dairy Products. 17th ed. Washington: American Public Health Association; 2004. p. 227–48.

147. Ryu D, Wolf-Hall C. Yeasts and molds. In: Salfinger Y, Tortorello ML, editors. Compendium of Methods for the Microbiological Examination of Foods. 5th ed. Washington; 2015. p. 277–86.

148. Kornacki J., Gurtler JB, Stawick BA. Enterobacteriaceae, coliforms, and Escherichia coli as quality and safety indicators. In: Salfinger Y, Tortorello ML, editors. Compendium of Methods for the Microbiological Examination

of Foods. 5th ed. Washington: American Public Health Association; 2015. p. 103–20.

149. ISO 6579:2002. Microbiology of food and animal feeding stuffs — Horizontal method for the detection of Salmonella spp. 4th ed. 2002. 27 p.
150. Chutia H, Mahanta CL. Influence of cold plasma voltage and time on quality attributes of tender coconut water (Cocos nucifera L.) and degradation kinetics of its blended beverage. J Food Process Preserv. 2021;45(4):1–12.
151. Ma Y, Xu L, Wang S, Xu Z, Liao X, Cheng Y. Comparison of the quality attributes of coconut waters by high-pressure processing and high-temperature short time during the refrigerated storage. Food Sci Nutr. 2019;7(4):1512–9.
152. Mahnot NK, Gupta K, Mahanta CL. Shelf life enhancement and associated quality and sensory changes on refrigerated storage of tender coconut water subjected to non-thermal microfiltration and treated with additives. J Food Sci Technol. 2019;56(7):3408–21.
153. Pandiselvam R, Prithviraj V, Manikantan MR, Beegum PPS, Ramesh S V., Kothakota A, et al. Dynamics of biochemical attributes and enzymatic activities of pasteurized and bio-preserved tender coconut water during storage. Front Nutr. 2022;9.
154. Ahmed J, Arfat YA, Al-Attar H, Auras R, Ejaz M. Rheological, structural, ultraviolet protection and oxygen barrier properties of linear low- density polyethylene films reinforced with zinc oxide (ZnO) nanoparticles. Food Packag Shelf Life [Internet]. 2017;13(April):20–6. Available from: http://dx.doi.org/10.1016/j.fpsl.2017.04.005

155. Villaluenga JPG, Seoane B. Influence of drawing on gas transport mechanism in LLDPE films. Polymer (Guildf). 1998;39(17):3955–65.

156. Tazeen H, Kannan M. Research Journal of Agricultural Sciences Changes in Gas Transmission Rate and Water Vapour Permeability in PP and LLDPE Nano Composite Films. Res J Agric Sci. 2019;(June).

157. Gouvea FS, Padilla-Zakour OI, Worobo RW, Xavier BM, Walter EHM, Rosenthal A. Effect of high-pressure processing on bacterial inactivation in açaí juices with varying pH and soluble solids content. Innov Food Sci Emerg Technol [Internet]. 2020;66(August):102490. Available from: https://doi.org/10.1016/j.ifset.2020.102490

158. Nguyen TT, Huynh Nguyen TT, Tran Pham BT, Van Tran T, Bach LG, Bui Thi PQ, et al. Development of poly (vinyl alcohol)/agar/maltodextrin coating containing silver nanoparticles for banana (Musa acuminate) preservation. Food Packag Shelf Life [Internet]. 2021;29(February):100740. Available from: https://doi.org/10.1016/j.fpsl.2021.100740

159. Vieira ACF, de Matos Fonseca J, Menezes NMC, Monteiro AR, Valencia GA. Active coatings based on hydroxypropyl methylcellulose and silver nanoparticles to extend the papaya (Carica papaya L.) shelf life. Int J Biol Macromol [Internet]. 2020;164:489–98. Available from: https://doi.org/10.1016/j.ijbiomac.2020.07.130